

AD-A067 582

NAVAL POSTGRADUATE SCHOOL MONTEREY CALIF  
SOME TESTS OF THE PENNSYLVANIA STATE UNIVERSITY MESOSCALE MODEL--ETC(U)  
DEC 78 M R HACUNDA

F/G 4/2

UNCLASSIFIED

1 OF 1  
AD  
A067582



NL



END  
DATE  
FILMED  
6 --79  
DDC

ADA067582

DDC FILE COPY

LEVEL #

2 NW

NAVAL POSTGRADUATE SCHOOL  
Monterey, California



THESIS



SOME TESTS OF THE PENNSYLVANIA  
STATE UNIVERSITY MESOSCALE MODEL  
WITH TROPICAL CYCLONES

by

Michael Richard Hacunda

December 1978

Thesis Advisor:

R. Elsberry

Approved for public release; distribution unlimited.

79 04 19 011

UNCLASSIFIED

SECURITY CLASSIFICATION OF THIS PAGE (When Data Entered)

REPORT DOCUMENTATION PAGE		READ INSTRUCTIONS BEFORE COMPLETING FORM
1. REPORT NUMBER	2. GOVT ACCESSION NO.	3. RECIPIENT'S CATALOG NUMBER
4. TITLE (and Subtitle) 6 Some Tests of the Pennsylvania State University Mesoscale Model with Tropical Cyclones.		5. TYPE OF REPORT & PERIOD COVERED 9 Master's Thesis, December 1978
7. AUTHOR(s) 10 Michael Richard Hacunda		8. PERFORMING ORG. REPORT NUMBER
9. PERFORMING ORGANIZATION NAME AND ADDRESS Naval Postgraduate School Monterey, California 93940		10. CONTRACT OR GRANT NUMBER(s) 12 81 p.
11. CONTROLLING OFFICE NAME AND ADDRESS Naval Postgraduate School Monterey, California 93940		12. REPORT DATE 11 December 1978
14. MONITORING AGENCY NAME & ADDRESS (if different from Controlling Office)		13. NUMBER OF PAGES 80
		15. SECURITY CLASS. (of this report) Unclassified
		16a. DECLASSIFICATION/DOWNGRADING SCHEDULE
16. DISTRIBUTION STATEMENT (of this Report) Approved for public release; distribution unlimited.		
17. DISTRIBUTION STATEMENT (of the abstract entered in Block 20, if different from Report)		
18. SUPPLEMENTARY NOTES		
19. KEY WORDS (Continue on reverse side if necessary and identify by block number) Pennsylvania State University Mesoscale Model Cyclone Prediction 251 450 Jm		
20. ABSTRACT (Continue on reverse side if necessary and identify by block number) A three-dimensional, primitive equation model by Anthes and Warner (1978) was used to predict five typhoon cases. The five-layer model on a 40X40 staggered grid with 120 km resolution included a moisture cycle, sensible and latent heat flux at the earth's surface, and a bulk parameterization of the planetary boundary layer. The model is initialized using operational wind fields and two forms of a wind bogus.		

DD FORM 1 JAN 73 1473  
(Page 1)EDITION OF 1 NOV 68 IS OBSOLETE  
S/N 0102-014-6601

UNCLASSIFIED

1 SECURITY CLASSIFICATION OF THIS PAGE (When Data Entered)

79 04 19 011

UNCLASSIFIED

SECURITY CLASSIFICATION OF THIS PAGE/When Data Entered:

ABSTRACT (Cont'd)

Due to the lack of a representative moisture analysis in the vicinity of tropical cyclones, simulated moisture fields were used to initialize the model. Initial experiments conducted with these fields produced widespread convection and heating which developed circulations in areas well removed from the actual storm. The associated modifications to the steering flow, and the overly intense storm circulations resulted in premature recurvature. Use of a second moisture bogus, which provided less available moisture (especially at upper levels), reduced the amount of convection over the entire grid and the effect on the steering current.

A second wind bogus based on a scheme described by Hovermale (1976) was also tested. This technique resulted in a smaller and less intense initial storm, which also resulted in considerably less convection. The tracks forecast by the different wind and moisture fields were compared with forecasts of the 60 km resolution Madala and Hodur model using the same initial data.

ACCESSION for	
DTIC	WRITE SECTION <input checked="" type="checkbox"/>
DOC	DOT SECTION <input type="checkbox"/>
UNCLASSIFIED	<input type="checkbox"/>
JUSTIFICATION	
BY	
DISTRIBUTION/AVAILABILITY CODE	
Dist.	AVAIL. AND SPECIAL
A	

DD Form 1473  
1 Jan 73  
S/N 0102-014-6601

UNCLASSIFIED

2 SECURITY CLASSIFICATION OF THIS PAGE/When Data Entered:



Approved for public release; distribution unlimited.

Some Tests of the Pennsylvania  
State University Mesoscale Model  
with Tropical Cyclones

by

Michael Richard Hacunda  
Lieutenant, United States Navy  
B.S., Pennsylvania State University, 1973

Submitted in partial fulfillment of the  
requirements for the degree of

MASTER OF SCIENCE IN METEOROLOGY & OCEANOGRAPHY

from the

NAVAL POSTGRADUATE SCHOOL  
December 1978

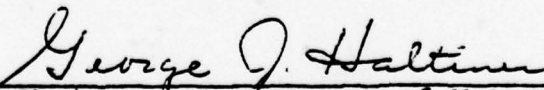
Author

  
\_\_\_\_\_

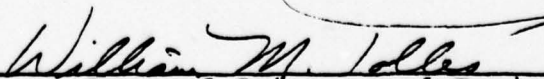
Approved by:

  
\_\_\_\_\_

Thesis Advisor

  
\_\_\_\_\_

Chairman, Department of Meteorology

  
\_\_\_\_\_

Dean of Science and Engineering

# ABSTRACT

A three-dimensional, primitive equation model by Anthes and Warner (1978) was used to predict five typhoon cases. The five-layer model on a 40X40 staggered grid with 120 km resolution included a moisture cycle, sensible and latent heat flux at the earth's surface, and a bulk parameterization of the planetary boundary layer. The model is initialized using operational wind fields and two forms of a wind bogus.

Due to the lack of a representative moisture analysis in the vicinity of tropical cyclones, simulated moisture fields were used to initialize the model. Initial experiments conducted with these fields produced widespread convection and heating which developed circulations in areas well removed from the actual storm. The associated modifications to the steering flow, and the overly intense storm circulations resulted in premature recurvature. Use of a second moisture bogus, which provided less available moisture (especially at upper levels), reduced the amount of convection over the entire grid and the effect on the steering current.

A second wind bogus, based on a scheme described by Hovermale (1976) was also tested. This technique resulted in a smaller and less intense initial storm, which also resulted in considerably less convection. The tracks forecast by the different wind and moisture fields were compared with forecasts of the 60 km resolution Madala and Hodur model using the same initial data.

## TABLE OF CONTENTS

I.	INTRODUCTION -----	12
II.	DESCRIPTION OF THE MODEL -----	13
III.	EXPERIMENTS -----	18
	A. RESULTS OF THE FIRST COMMON EXPERIMENT ----	18
	B. MOISTURE EXPERIMENTS -----	20
	C. RESULTS OF RH-BOGUS 2 -----	21
	D. NO HEAT EXPERIMENT -----	22
	E. CHANGES TO THE MODEL -----	22
	F. HORIZONTAL DIFFUSION EXPERIMENT -----	26
	G. WIND BOGUS EXPERIMENTS -----	28
	H. RESULTS OF WIND BOGUSING EXPERIMENTS -----	31
IV.	COMPARISON WITH OTHER MODELS -----	33
V.	CONCLUSIONS -----	40
	ILLUSTRATIONS -----	43
	APPENDIX A -----	77
	LIST OF REFERENCES -----	78
	INITIAL DISTRIBUTION LIST -----	79

LIST OF TABLES

<u>Table #</u>	<u>Caption</u>	<u>Page</u>
1	Fractions used for condensing excess moisture to obtain 100% relative humidity -----	15
2	Relative humidities used in Rh-bogus 1 and Rh-bogus 2 -----	17
3	Revised values of the vertical distribution of latent heating, $N(\sigma)$ ---	24
4	Summary of experiments using the various bogusing techniques -----	33
5	Summary of position vector errors -----	36



# LIST OF ILLUSTRATIONS

Figure #	Caption	Page
1	Typhoon KIM 24-h forecast VT 77111012 600 mb winds ( $\text{m s}^{-1}$ ) and relative humidity (coordinates are grid points vice latitude and longitude) -----	43
2	Typhoon KIM 48-h forecast VT 77111112 150 mb winds ( $\text{m s}^{-1}$ ) and relative humidity (isoline spacing is 20%) -----	44
3a	Typhoon KIM initial field SLP-1000 mb and winds ( $\text{m s}^{-1}$ ) at $\sigma = .95$ using V- bogus 1 (isoline spacing is 4 mb) -----	45
3b	Typhoon KIM 12-h forecast SLP-1000 mb and winds ( $\text{m s}^{-1}$ ) at $\sigma = .95$ using V- bogus 1 and Rh-bogus 1 -----	46
3c	Typhoon KIM 24-h forecast SLP-1000 mb and winds ( $\text{m s}^{-1}$ ) at $\sigma = .95$ using V- bogus 1 and Rh-bogus 1 -----	47
3d	Typhoon KIM 36-h forecast SLP-1000 mb and winds ( $\text{m s}^{-1}$ ) at $\sigma = .95$ using V- bogus 1 and Rh-bogus 1 -----	48
4	Typhoon OLIVE 36-h forecast VT 78042300 SLP-1000 mb and winds ( $\text{m s}^{-1}$ ) at $\sigma = .95$ using V-bogus 1 and Rh-bogus 1 -----	49
5	Typhoon OLIVE 36-h forecast VT 78042300 accumulated convective precipitation (cm) using V-bogus 1 and Rh-bogus 1. Center value of Olive is 20 cm (isoline spacing is 1 cm) -----	50
6	Typhoon OLIVE 36-h forecast VT 78042300 convective heating ( $^{\circ}\text{C}/\text{day}$ ) using V- bogus 1 and Rh-bogus 1 (isoline spacing is 25 $^{\circ}\text{C}/\text{day}$ ) -----	51
7	Typhoon OLIVE 36-h forecast VT 78042300 SLP-1000 mb and winds ( $\text{m s}^{-1}$ ) at $\sigma = .95$ using V-bogus 1 and Rh-bogus 2 -	52

Figure #	Caption	Page
8	Typhoon OLIVE 36-h forecast VT 78042300 accumulated convective precipitation (cm) using V- bogus 1 and Rh-bogus 2 -----	53
9	Typhoon OLIVE 36-h forecast VT 78042300 convective heating ( $^{\circ}\text{C}/\text{day}$ ) using V-bogus 1 and Rh-bogus 2 -----	54
10a	Typhoon KIM 12-h forecast VT 77111000 accumulated convective precipitation (cm) using V-bogus 1 and Rh-bogus 1 before making changes to model constants (see text) -----	55
10b	Typhoon KIM 12-h forecast VT 77111000 accumulated convective precipitation (cm) using V-bogus 1 and Rh-bogus 1 after changes to model constants (see text) -----	56
10c	Typhoon KIM 12-h forecast VT 77111000 convective heating ( $^{\circ}\text{C}/\text{day}$ ) before changes to model constants (see text) -----	57
10d	Typhoon KIM 12-h forecast VT 77111000 convective heating ( $^{\circ}\text{C}/\text{day}$ ) using V-bogus 1 and Rh-bogus 1 after changes to model constants (see text) -----	58
11	Typhoon KIM 24-h forecast VT 77111012 SLP-1000 mb and winds ( $\text{m s}^{-1}$ ) at $\sigma = .95$ without convec- tive heating effects -----	59
12a	Typhoon KIM initial SLP-1000 mb and winds ( $\text{m s}^{-1}$ ) at $\sigma = .95$ using V-bogus 1 -----	60
12b	Typhoon KIM initial SLP-1000 mb and winds ( $\text{m s}^{-1}$ ) at $\sigma = .95$ using V-bogus 3 -----	61
12c	Typhoon KIM initial winds ( $\text{m s}^{-1}$ ) at 400 mb using V-bogus 1, and relative humidity (Rh-bogus 1) -----	62

Figure #	Caption	Page
12d	Typhoon KIM initial winds ( $\text{m s}^{-1}$ ) at 400 mb using V-bogus 3 -----	63
13	Typhoon KIM 12-h forecast VT 77111000 SLP-1000 mb and winds at $\sigma = .95$ using V-bogus 3 and Rh-bogus 2 -----	64
14	Typhoon KIM 12-h forecast VT 77111000 accumualted convective precipitation (cm) using V-bogus 3 and Rh-bogus 2 -----	65
15	Typhoon KIM 12-h forecast VT 77111000 convective heating ( $^{\circ}\text{C/day}$ ) using V-bogus 3 and Rh-bogus 2 -----	66
16	Forecast tracks of Typhoon KIM for V-bogus 1 versus V-bogus 3 using Rh-bogus 2 and the Penn State model --	67
17	Forecast tracks of Typhoon OLIVE (78042400) using the Penn State (PSU), split semi-implicit (SSI) and Channel (Ch) models -----	68
18	Forecast tracks of Typhoon OLIVE (78042400) using the Penn State (PSU), split semi-implicit (SSI) and Channel (Ch) models -----	69
19	Forecast tracks of Typhoon KIM (77110912) using the Penn State (PSU), split semi-implicit (SSI) and Channel (Ch) models -----	70
20	Forecast tracks of Typhoon PAMELA (76051900) using the Penn State (PSU), split semi-implicit (SSI) and Channel (Ch) models -----	71
21	Forecast tracks of Typhoon PAMELA (76052200) using the Penn State (PSU), split semi-implicit (SSI) and Channel (Ch) models -----	72
22	Typhoon PAMELA (76052200) initial SLP-1000 mb and winds ( $\text{m s}^{-1}$ ) at $\sigma = .95$ using V-bogus 1 -----	73



Figure #	Caption	Page
23	Typhoon PAMELA (76052200) initial SLP-1000 mb and winds ( $\text{m s}^{-1}$ ) using high intensity version of V-bogus 3 (V-bogus 4) -----	74
24	Plot of vorticities produced by V-bogus 1, V-bogus 3, and high intensity V-bogus 3 (V-bogus 4) -----	75
25	Forecast track of PAMELA (76052200) using V-bogus 4 versus V-bogus 1 and V-bogus 3 in the Penn State (PSU) model -	76



### ACKNOWLEDGMENTS

The research was accomplished using facilities provided by Fleet Numerical Weather Center (FNWC), Monterey, California. The use of these facilities and the concern and advice provided by the personnel of the Computer Systems department is greatly appreciated.

The advice and considerable assistance offered by Richard Hodur of the Naval Environmental Prediction Research Facility (NEPRF) is greatly appreciated. His initialization scheme, data, and his help in programming were invaluable.

Finally, I would like to express my thanks to R.A. Anthes and R.L. Elsberry. Without their encouragement, advice and direction, this research would have been impossible.

## I. INTRODUCTION

The major objective of this set of experiments was to test a general mesoscale model using operationally-analyzed data to determine effectiveness in forecasting tropical cyclone development and movement compared to some other tropical cyclone models currently being tested. The Penn State model was selected because it contained boundary layer physics, a convective moisture cycle, and other options which could be easily included in (or excluded from) any forecast. It was then possible to determine the effects and relative importance of the various parameterizations by selectively incorporating different combinations. This model was also chosen for its general code which allowed changes to be made easily to the resolution and size of the vertical and horizontal domains. These changes were necessitated by time and computer availability constraints.

During the initial forecasts, it was discovered that the initial wind and moisture conditions played a very important role in determining the development and movement of tropical cyclones. An investigation was then conducted to determine the extent of the effects of the initial wind and moisture conditions on the model forecasts. This paper presents the results of these experiments and compares forecasts made using the Penn State model with forecasts made using two other tropical cyclone models.

## II. DESCRIPTION OF THE MODEL

The experiments used a general, three-dimensional, primitive equation model designed to forecast flows with characteristic wavelengths of 10-2500 km. Provisions of the model included a variable terrain, a moisture cycle, latent heating, sensible heat flux at the earth's surface and boundary layer physics. The moisture cycle modeled both stable (nonconvective) precipitation with grid-scale relative humidities in excess of 100%, and unstable (convective) precipitation with grid-scale relative humidities less than 100%. Details, such as the finite difference equations and staggered grid lattice, were retained intact as described by Anthes and Warner (1978).

The particular version of the model used in this set of experiments was similar to one described by Anthes (1978). Model inputs consisted of pressure weighted wind components ( $p \cdot u, p \cdot v$ ), relative humidity and temperature at five levels, surface pressure, sea surface temperature and terrain. Predicted parameters were wind components ( $u, v$ ), surface pressure ( $p_s$ ), relative humidity (moisture), and potential temperature ( $\theta$ ). Anthes's (1978) version was reduced from 7 levels to 6 levels at which  $\sigma$  was defined ( $\sigma = 0.0, 0.3, 0.5, 0.7, 0.9$  and  $1.0$ ) with all other variables ( $V, T, \phi, \omega$ , and  $q$ ) defined halfway between these levels at  $\sigma = 0.15, 0.4, 0.6, 0.8$  and  $0.95$ . Sigma level 0.0 corresponded



to a pressure of 0 millibars. To reduce computer time, a 40x40 grid in Mercator coordinates with 120 km resolution was selected rather than the 50x50 grid with 60 km resolution used by Anthes (1978). Other simplifications were made to the model for economic reasons as described by Anthes (1978). A spatially and temporally constant vertical distribution of latent heating associated with cumulus convection was specified in lieu of a one-dimensional cloud model (Anthes, 1977), and a simplified version of Deardorff's (1972) bulk parameterization of the planetary boundary layer (PBL) was substituted for the high resolution PBL (Anthes and Warner, 1978). This scheme assumed that the surface wind,  $|\underline{v}_s|$ , was equal to the wind at the lowest level ( $\sigma = 0.95$ ). All experiments described here used an ocean terrain with no land, and as such, a constant value of  $1.5 \times 10^{-3}$  was used for the drag coefficient,  $C_D$ .

All layers were checked for supersaturation and  $\theta$  and  $q$  were adjusted to maintain relative humidities less than 100% by condensing a fraction of the moisture excess and adding the associated latent heat to the temperature tendency. The original model assumed a constant fraction of .31 for all levels. This factor was modified using an approximation suggested by Haltiner (personal communication). A new constant was calculated for each level using the equation

$$\Delta q = \frac{q_s - q}{[1 + L^2 q_s / C_p R_v T^2]} \quad (1)$$



where typical values for  $q$  and  $T$  were obtained from Jordan's (1958) mean September tropical sounding and Sheets' (1969) mean hurricane sounding. The modified values which were equal to the reciprocal of the denominator in equation (1) are listed in Table 1.

Initial conditions were derived from the Fleet Numerical Weather Central (FNWC) Global Band Analysis. Initialization was accomplished using a scheme developed by Hodur (personal communication) for use with the Madala and Hodur (1977) split semi-implicit tropical cyclone model. This scheme used a reverse balancing technique to derive interior geopotential values on sigma levels from the nondivergent wind components using a nonlinear balance equation. Balancing was conducted over a  $51 \times 51$  grid with 120 km resolution, from which the  $40 \times 40$  grid was interpolated for input to the model.

Table 1. Fractions used for condensing excess moisture to obtain 100% relative humidity. Values for  $T$  and  $q$  were taken from representative tropical soundings. Values of  $q_s$  were calculated using the Clausius-Clapeyron equation.

Level ( $\sigma$ )	$T$ ( $^{\circ}\text{K}$ )	$q_s$ ( $\text{gkg}^{-1}$ )	Fraction
0.15	206.76	0.0433	0.986
0.40	258.26	3.0399	0.619
0.60	275.66	7.6894	0.422
0.80	286.36	12.0868	0.335
0.95	295.76	18.8008	0.256

Initial wind conditions were composed of both analyzed and idealized values. Following Hodur (personal communication), a symmetrical wind bogus (referred to as V-bogus 1) was obtained within a 360 km radius of the storm center by adding idealized values to the vorticity field (which was derived from the analyzed winds) prior to calculation of the stream function and nondivergent winds. Bogus vorticity values were calculated for the surface to 700 mb from

$$\zeta(k) = \frac{2V_{\max}}{r_0}, \quad (2)$$

where  $V_{\max}$  was the magnitude of the wind at the radius of maximum wind ( $r_0$ ). The vorticity maximum at 100 mb was set equal to  $1.0 \times 10^{-5} \text{ s}^{-1}$ , with the vorticity at intermediate levels varied linearly between 700 mb and 100 mb. Horizontally, the vorticity was decreased in accordance with

$$\zeta_r(k) = \zeta_{\max}(k) e^{-r/90}, \quad 0 \leq r \leq 360 \quad (3)$$

where  $r$  was the radial distance (km) from the storm center. Values for  $V_{\max}$  were taken from Typhoon Reports and typhoon warning messages and the radius of maximum wind (RMW),  $r_0$ , was set equal to 60 km.

Due to the lack of representative moisture analyses in the vicinity of tropical cyclones, idealized moisture fields

(referred to as Rh-bogus 1) were used to initialize the model. These fields were produced by specifying a uniform field of large scale relative humidities which decreased with height. Further bogusing of the storm was accomplished by centering a five grid point square of higher relative humidities, which also decreased with height, over the storm. In this manner, the storm started with more moisture than the surrounding environment. Large scale and storm relative humidities are given in Table 2.

Table 2. Relative humidities used in Rh-bogus 1 and Rh-bogus 2

Level ( $\sigma$ )	Storm	Large Scale
0.15	.80	.50
0.40	.80	.60
0.60	.90	.70
0.80	.90	.80
0.95	.95	.85

Relative humidities used in Rh-bogus 2.

Level ( $\sigma$ )	Storm		Large Scale
	low	high	
0.15	.30	.40	.20
0.40	.53	.60	.46
0.60	.76	.87	.51
0.80	.77	.87	.69
0.95	.80	.90	.80



### III. EXPERIMENTS

The basic experiment consisted of 48-hour forecasts for the following five cases using all of the model's options (with the exception of terrain);

- I. Typhoon OLIVE 78042112 (year,month,day,12 GMT)
- II. Typhoon OLIVE 78042400
- III. Typhoon KIM 77110912
- IV. Typhoon PAMELA 76051900
- V. Typhoon PAMELA 76052200.

Tracks of these storms were then compared to the tracks obtained from forecasts made with the Madala and Hodur (1977) split semi-implicit (SSI) model, the FNWC Operational Tropical Cyclone (Channel) model (Mihok and Hinsman, 1977), and the best track analyses. Appendix A contains a comparison of these two models with the Penn State model. Further experiments were then conducted to test the model's sensitivity to the initial wind and moisture conditions and to the convective parameterization.

#### A. RESULTS OF THE FIRST COMMON EXPERIMENT

All five cases experienced strong recurvature. See Figs. 17 through 21 for positions relative to the best track. Examination of the wind and moisture fields revealed several characteristics which were common to all cases. Every storm developed strong frictional convergence with large cross-isobaric flows at low levels, even in areas of high wind



velocities. Although the maximum storm intensities varied, all five cases developed a southerly flow at middle levels just to the east of the storm. An example of this circulation, which was especially prevalent at 600 mb for Typhoon KIM, can be seen in Fig. 1. A tendency to produce a large anticyclonic circulation at 150 mb with strong westerlies located along the northern branch of the gyre also existed in all cases. An example of this circulation is given in Fig. 2. This circulation, combined with the strong middle level southerly flow, probably contributed significantly to recurving the storms.

Another dominant characteristic common to all cases, which contributed to the recurvature effect, was the production of widespread convection, with particularly strong convective activity occurring after 12 to 24 hours in the northeast corner and along the northern boundary. All cases experienced excessive vertical velocities accompanied by strong latent heating and precipitation (both convective and nonconvective) in these areas, which resulted in the formation of localized areas of lower pressures. Continued development of a trough in the northeast corner distorted the entire surface pressure pattern to such an extent that the storm was steered toward the corner, producing even greater development in this region and more rapid recurvature of the storm. An example of this sequence can be seen in Figs. 3a through 3d. Forecasts for both cases of Typhoon OLIVE also developed severe convection in the

southwest corner and an intense circulation was produced between 24 and 36 hours. The first OLIVE case also developed an additional circulation which had existed initially to the west of the storm. An example of the areas which underwent development due to convective activity can be seen in Figs. 4 through 6. The development of these circulations near the boundaries prompted an investigation into the moisture fields, latent heat parameterization scheme and the boundary conditions. These topics are examined in the following sections. The general procedure was to select a typical case and examine successively the effect of each modification on that storm. After adopting the modifications based on the one case, the entire set of five cases was re-run.

#### B. MOISTURE EXPERIMENTS

A new moisture initialization was introduced in an attempt to reduce the amount of convection and high relative humidities at upper levels in regions not associated with the storm. The second technique (referred to as Rh-bogus 2) also consisted of an area of higher relative humidities superimposed on a uniform field of lower values. However, the second moisture bogus covered an area with a radius of 3 grid points (360 km), which was the same area covered by the wind bogus. The large scale values, which were based on Jordan's (1958) mean September tropical sounding, varied only with height, while the storm relative humidities,

taken from Sheet's (1969) mean hurricane sounding, depended on the storm surface pressure as well as height. Values used in this scheme are listed in Table 2. The high range of relative humidities was used for storm surface pressures less than 995 mb and the low set for pressures greater than 1014 mb, with a linear interpolation between those sets for intermediate storm surface pressures. Note that the major difference in Rh-bogus 2 was the reduction of all relative humidities, especially at upper levels. Additional 48-hour forecasts were then conducted for both cases of OLIVE using the new moisture bogus. OLIVE was chosen because it had the most widespread convection of all the cases.

#### C. RESULTS OF RH-BOGUS 2

The results of the low moisture bogus are typified in Figs. 7 through 9. Convective activity was reduced over the entire grid with the greatest effect noticeable in the reduced development of those areas not associated with the storm. The total convective rain produced over the grid was reduced from 382 cm to 198 cm, while the total non-convective precipitation was reduced from 26 cm to 7 cm in the first 12 hours. More significant, however, was the reduction of the maximum convective precipitation associated with the second cyclone (located to the west of OLIVE) from 12.5 cm to 1.4 cm. The maximum convective precipitation associated with OLIVE was only reduced from 5.9 cm to 4.5 cm.



The associated convective heating rate at 12 hours was lowered from 280 °C/day to 60 °C/day over the second cyclone, while the heating over OLIVE was reduced from 160 °C/day to 110 °C/day. Similar results were obtained in the other areas, particularly in the northeast corner, although the development of the trough in this region was not prevented.

The net effects of the low moisture bogus were filling the storm by about 2 mb and decreasing the winds by less than 10%, while significantly reducing the deepening over the large scale areas. The general characteristics of the flow were not altered, nor were the forecast tracks significantly altered.

#### D. NO HEAT EXPERIMENT

A 24-hour forecast was then made using the high humidity bogus, but without including latent heating effects in the temperature prediction equation. Typhoon KIM was chosen for this experiment because it had the best predicted track of the five cases using the SSI model and had been used with and without the wind bogus (Hodur, personal communication). Deletion of latent heating effects (due both to convective and nonconvective processes) resulted in rapid filling of the storm and only marginal improvement of the storm track.

#### E. CHANGES TO THE MODEL

Before continuing with further experiments, several detailed changes were made to some of the model-defined



constants to make the 5-layer version more closely resemble the original 6-layer model described by Anthes (1978). The vertical distribution of convective heating,  $N(\sigma)$ , defined by Anthes (1977), was altered in the lowest two layers such that the same amount of heating was provided, but over different layer thicknesses. Because this function was normalized, the changes produced in these two layers were distributed throughout the vertical. The corrected values of  $N(\sigma)$ , which provided the same distribution of convective heating described by Anthes (1978) in the 6-layer model, are compared in Table 3. A 24-hour forecast using the high moisture bogus and the revised heating distribution produced a 10% reduction in convection and its associated latent heating and precipitation. The storm center filled 1 mb.

Two other changes were made to the convective parameterization. The vertical eddy fluxes,  $\delta\omega_c(q_c - \bar{q})/\delta\sigma$ , which determined  $\partial q/\partial t$  in the cloud, were altered to make the vertical distribution of cloud moisture more representative of the distribution outlined by Anthes (1977). A 24-hour forecast produced less convection, precipitation, and heating, and increased the surface pressure of the storm by 1 mb. Convection over the entire grid was further reduced in a 12-hour forecast by increasing the critical value of the integrated water vapor convergence,  $M_t$ , required for convection to occur from  $3.0 \times 10^{-7}$  to  $3.0 \times 10^{-6} \text{ g H}_2\text{O m}^{-2}\text{s}^{-1}$  where

Table 3. Revised values of the vertical distribution of latent heating,  $N(\sigma)$ . (New values are given for experiment designed to shift heating maximum to higher levels.)

Level (mb)	6-layer	5-layer	New
150	-	.375	.7595
300	1.065	-	
400	-	1.5	1.5190
460	1.308	-	
580	1.356	-	
600	-	1.625	1.2658
700	1.162	-	
800	-	1.25	1.0126
820	.872	-	
940	.194	-	
950	-	.125	.1266

$$M_t = -\frac{1}{g} \sum_{k=k_1}^k \nabla \cdot (p^* \tilde{V} q) \delta \sigma_k + \frac{1}{g} (p^* q \dot{\sigma})$$

The number of grid points experiencing convection for any one time step was reduced significantly, with the maximum number of grid points (at 12-hours) lowered from 797 to only 222. The total convective precipitation over the grid was reduced from 414 cm to 263 cm. The changes in convective precipitation and heating produced by the revisions discussed here, can be seen in Figs. 10a through 10d. Although the motivation for the above changes was to reduce what appeared to be excessive latent heating in the model, note that the circulation in the northeast corner still experiences strong convergence and excessive precipitation.

Two experiments designed to test the model's sensitivity to the convective parameterization were conducted using Rhobogus 2 for initial conditions. A 24-hour forecast was made using a vertical distribution of latent heating which shifted the maximum heating to higher levels. This was done so that the model would develop more cyclonic circulation at upper levels and possibly produce a greater westward movement. The new values of  $N(\sigma)$  are listed in Table 3. Additional upper level heating produced less precipitation in the northeast corner but failed to alter the forecast significantly in 24-hours. Another 24-hour forecast was made with the integrated water vapor convergence,  $M_t$ ,

calculated for only the two lowest layers of the model. The objective of this experiment was to remove the effects of the large upper level moisture convergence and, thereby, reduce the precipitation in the northeast corner while not seriously affecting the storm. Confinement of the moisture convergence calculation to low levels reduced convection and development of a trough in the northeast corner while intensifying convection associated with the storm after 12 hours. However, after 24 hours, the trough in the northeast corner developed rapidly and produced results similar to those already encountered. These last two model revisions were not incorporated into the model for future experiments.

Frictional effects were also modified for changes made in  $\delta\sigma$  and  $p^*$  which had resulted from changing the pressure at the top of the model from 200 mb to 0 mb, and decreasing the thickness of the surface layer from 150 mb to 100 mb. These modifications resulted in a 4% decrease in the effective drag coefficient. A 12-hour forecast made using the reduced friction deepened the storm surface pressure by 1 mb and increased the amount of convection occurring over the storm, while decreasing the total number of grid points experiencing convection.

#### F. HORIZONTAL DIFFUSION EXPERIMENT

An attempt was made to reduce the strong horizontal shears which existed along the boundaries. An example of



this shear can be seen in Fig. 2 where the interior upper level circulation differs drastically from the conditions along the western and southern boundaries. Since this characteristic also occurred when the model was run with extratropical data (see Anthes, 1978, Figs. 23c through 23e), it was decided to increase the horizontal diffusion. The horizontal eddy viscosity,  $K_H$ , was multiplied by an amplification factor which increased from a value of 1.0 near the center to a maximum near the boundaries, where  $K_H$  was restricted to be less than  $30 \times 10^4 \text{ m}^2 \text{ s}^{-1}$ . All future runs with the model were made using twice the calculated  $K_H$  and a maximum value of  $60 \times 10^4 \text{ m}^2 \text{ s}^{-1}$ . The increased diffusion decreased the shears along the boundaries by less than 10% and therefore did not significantly reduce the convergence which resulted in convection along the northern and eastern boundaries.

Another factor which may have contributed to overdevelopment of the northeast corner was the lack of moisture diffusion. The winds, especially at upper levels, tended to advect moisture into that corner. Without diffusion, it may have been possible that moisture simply accumulated in the corner producing more convection. This effect can be seen by comparing Fig. 3c with Fig. 11 which is the 24-hour forecast without latent heating. In the latter, although convection occurred, the heating effects were not added to the tendency and the circulation near the corner did not

develop. As a result, the surface pressure pattern was not distorted.

#### G. WIND BOGUS EXPERIMENTS

As demonstrated in Fig. 3a, the initial wind bogus (V-bogus 1) produced a storm which was very large. Although bogused values were entered in the vorticity field within a radius of 3 grid points, the cyclonic circulation and the associated pressure fields derived from the balance equation extended out to a radius of 8-10 grid points. It was also desirable to include an inner region of cyclonic outflow at upper levels. A second wind bogus (V-bogus 2) was calculated using the same conditions from the surface to 700 mb as V-bogus 1, while at 400 mb, the vorticity was given by

$$\zeta_r = \zeta_{\max} - \frac{r}{180}(\zeta_{\max} + f) \quad r < 180 \text{ km}, \quad (4)$$

$$\zeta_r = -f \quad r = 180 \text{ km}, \quad (5)$$

$$\zeta_r = -f + \frac{(r-180)}{180} f \quad 180 < r < 360 \text{ km}, \quad (6)$$

$$\zeta_r = 0 \quad r = 360 \text{ km}, \quad (7)$$

where the vorticity maximum,  $\zeta_{\max}$  was computed in the same manner as described earlier for V-bogus 1. At 100 mb, the vorticity was calculated using one-half the calculated

values for 400 mb. The vorticity at other levels (500, 300, 250, 200, and 150 mb) was varied linearly between 700 and 400 mb and between 400 and 100 mb. This bogus produced essentially the same results as V-bogus 1, probably because the circulation in the lowest levels of the storm was still very large.

Therefore, a third wind bogus (V-bogus 3) was calculated in an attempt to reproduce a wind bogus described by Hovermale et al (1976). The tangential wind,  $v_{\theta}$ , was calculated from

$$v_{\theta} (\text{m s}^{-1}) = \frac{22 r}{60} \quad 0 < r < 60 \text{ km}, \quad (8)$$

and

$$v_{\theta} (\text{m s}^{-1}) = 22 - \frac{(r-60 \text{ km})}{400 \text{ km}} 10$$

$$60 \leq r_1 \quad (9)$$

for the lowest level, while the upper level wind was derived using

$$v_{\theta} (\text{m s}^{-1}) = \frac{12 r}{60} \quad 0 < r < 60 \text{ km}, \quad (10)$$

$$v_{\theta} (\text{m s}^{-1}) = 12 \left[ 1 - \left( \frac{r-60}{300} \right) \right] \quad 60 \leq r < 660 \text{ km}, \quad (11)$$

and

$$v_{\theta} (\text{m s}^{-1}) = -12 \left[ 1 + \frac{(r-60 \text{ km})}{600 \text{ km}} \right] \quad 660 \leq r, \quad (12)$$

where  $r$  extended out to a radius of 6.4 grid points (768 km). The vorticity was then calculated from

$$\zeta = \frac{\partial v_{\theta}}{\partial r} + \frac{v_{\theta}}{r} - \frac{1}{r} \frac{\partial v_r}{\partial \theta} \quad (13)$$

where the last term was taken as zero for a symmetrical storm. Prior to substituting the bogused vorticity values, a simple Laplacian smoother was passed 30 times over the analyzed wind components in the same area covered by the bogus. Experiments conducted on both V-bogus 1 and V-bogus 3 with and without the smoother did not produce significantly different results for either bogus.

The following experiments were then conducted using Typhoon KIM and Rh-bogus 2;

- I. V-bogus 1: 24-hours
- II. V-bogus 3: 48-hours
- III. V-bogus 1 with one-half the vorticity maximum at the surface as in case I: 48-hours.

Differences produced in the initial wind fields by the two bogusing techniques can be seen in Fig. 12a through 12d. Note that V-bogus 1 produced a very large and intense storm compared to the one produced by V-bogus 3. In particular,



V-bogus 1 produced large changes in the winds and pressures at grid points a considerable distance from the storm. Because the 40x40 grid was selected from the interior of a 51x51 grid, wind values were changed as much as 50% in magnitude and 180° in direction along the boundaries by V-bogus 1. Subsequent analysis fields, that were required for calculation of the time-varying boundary values, were not bogused. The differences in these two fields introduced accelerations greater than expected in a 12-hour period along the southern and eastern boundaries. These accelerations were not introduced by V-bogus 3.

#### H. RESULTS OF WIND BOGUSING EXPERIMENTS

After 12 hours, V-bogus 1 produced convection at 100-200 grid points while V-bogus 3 produced convection at only 20-30 grid points. Total convective precipitation over the grid was lowered from 150 cm to 96 cm and the total stable rainfall was reduced by about 40%. V-bogus 3 dramatically reduced the amount of precipitation and heating in the northeast corner while concentrating more rain and heating over the storm. The effects of the smaller vortex can be seen in Figs. 13 through 15. Note the lack of development of a large trough in the northeast corner. The southerly flow at middle levels was also reduced. Reduced development of these two features resulted in the improved forecast track, shown in Fig. 16.

The 24-hour forecast developed more convection in the northeast corner, however the storm seemed to be sufficiently far from the corner to not be seriously affected by the weak troughing. A large anticyclonic circulation developed at 150 mb with strong southerly winds in the southwest quadrant. Apparently, these winds contributed to the northward movement of the storm.

Reducing the vorticity of V-bogus 1 to half the original value (Experiment III) resulted in a smaller vortex which produced values of convective activity, precipitation and heating which were between those produced by V-bogus 3 and the high intensity V-bogus 1. The track forecast using this bogus was also between the tracks produced by the other two boguses. This experiment demonstrated the effect that variations in the Coriolis parameter can have upon excessively large or intense vortices; that is, larger storms produce larger northward accelerations (Hovermale, et al., 1977).

#### IV. COMPARISON WITH OTHER MODELS

The effects of V-bogus 1 were compared to the FNWC analyzed fields (no storm bogus) for KIM, OLIVE (78042400) and PAMELA (76052200) using the SSI model by Hodur (personal communication). A 48-hour forecast was also made for PAMELA (76052200) using the high humidity moisture bogus (Rh-bogus 1) and V-bogus 1. A summary of the five cases available for comparison with experiments using the Penn State model is given in Table 4.

Table 4. Summary of experiments using the various bogusing techniques.

<u>Storm</u>	<u>SSI</u>	<u>Penn State</u>
OLIVE (78042112)	Analyzed winds, dry	V-bogus 1/Rh-bogus 1 V-bogus 3/Rh-bogus 2
OLIVE (78042400)	Analyzed winds, dry V-bogus 1, dry	same as above
KIM	Analyzed winds, dry V-bogus 1, dry	same as above
PAMELA (76051900)	Analyzed winds, dry	same as above
PAMELA (76052200)	Analyzed winds, dry V-bogus 1, dry V-bogus 1, wet	same as above

Forecast tracks obtained from the common experiments are shown in Figs. 17 through 21. V-bogus 1 produced more recurvature in all cases tested with the SSI model, although



not as much as it did in the Penn State model. The SSI model did not forecast the troughing that the Penn State model did in the northeast corner, although an area of lower surface pressure did exist there. The 12-hour forecast using the SSI scheme for KIM and PAMELA developed strong southerly flows to the east of the storm at middle levels which were similar to those produced by the Penn State model using V-bogus 1. However, the SSI model also developed strong northerly flows to the west of both storms at middle and upper levels. These winds acted to reduce the northward movement of the storm. The lack of the northerly winds, coupled with the trough in the northeast corner and the strong upper level anticyclone, allowed the southerly winds to move the storm a greater distance to the north in the Penn State model.

V-bogus 3 and Rh-bogus 2 decreased the upper level anticyclonic flow and strong southerly flow in all cases using the Penn State model. Although all cases continued to experience convection in the northeast corner and along the northern boundary, development of a strong trough was reduced and limited to forecast times in excess of 24 hours. Use of V-bogus 3 and Rh-bogus 2 resulted in improved tracks for all cases using the Penn State model. Insertion of V-bogus 1 in the SSI model reduced the errors in storm track positions for OLIVE and PAMELA and increased the errors for KIM (Hodur, personal communication). Rh-bogus 1

improved the forecast positions in the SSI model for PAMELA slightly over those using V-bogus 1 without moisture effects.

The Penn State model produced smaller errors than the SSI model in storm positions at 12 hours for most of the five cases. After 12 hours, the Penn State model using V-bogus 3 and Rh-bogus 2 produced smaller errors than the SSI using FNWC analyzed winds (no bogus), but larger errors than the SSI with V-bogus 1. The exception was Typhoon KIM for which all versions of the SSI scheme produced smaller errors than the Penn State model after 12 hours. Position vector errors are summarized in Table 5.

Finer resolution was probably responsible for the overall better accuracy obtained with the SSI model. The improved resolution allowed the storm to interact with small-scale circulations. With less resolution in the Penn State model, the large vortex storm was subjected primarily to the large-scale steering currents, and particularly more steering by the westerlies at upper levels, and consequently, more recurvature.

Both cases of PAMELA produced large errors in later forecasts due to insufficient recurvature when V-bogus 3 was used for initialization. The lack of recurvature probably resulted from the rapid filling and deterioration of storm structure which existed in all experiments using PAMELA. Observational data indicated that the maximum wind speed in the storm was much more intense ( $60 \text{ m s}^{-1}$ ),

Table 5. Summary of position vector errors (errors are in nautical miles)

Model	(h)	Storm				
		Olive (2112)	Olive (2400)	Kim (0912)	Pamela (1900)	Pamela (2200)
Channel						
	12	34	143	19	138	89
	24	124	303	106	227	133
	36	182	548	198	334	152
	48	398	743	230	475	228
SSI (analyzed winds, dry)						
	12	54	137	98	54	59
	24	94	400	59	177	173
	36	103	673	32	271	240
	48	210	892	43	356	326
SSI (V-bogus 1, dry)						
	12	-	52	69	-	65
	24	-	81	90	-	151
	36	-	-	103	-	195
	48	-	-	56	-	259
SSI (V-bogus 1, Rh-bogus 1)						
	12	-	-	-	-	31
	24	-	-	-	-	105
	36	-	-	-	-	125
	48	-	-	-	-	186
PSU (V-bogus 1, Rh-bogus 1)						
	12	74	52	36	85	39
	24	222	95	269	241	81
	36	332	290	527	368	228
	48	503	510	699	-	394



Table 5. (Cont'd)

Model	(h)	Olive (2112)	Olive (2400)	Kim (0912)	Pamela (1900)	Pamela (2200)
PSU (V-bogus 3, Rh-bogus 2)	12	38	29	36	44	12
	24	90	129	151	100	153
	36	151	280	159	182	197
	48	309	369	150	356	363
PSU (V-bogus 4, Rh-bogus 2)	12	-	-	-	-	12
	24	-	-	-	-	31
	36	-	-	-	-	129
	48	-	-	-	-	153

yet V-bogus 3 was designed to produce maximum winds of  $22 \text{ m s}^{-1}$ . Accordingly, V-bogus 3 was altered to include more intense wind speeds by changing equations (8) and (9) to

$$v_{\theta} (\text{m s}^{-1}) = 60 \frac{r}{60} \quad 0 < r < 60 \text{ km} \quad (14)$$

and

$$v_{\theta} (\text{m s}^{-1}) = 60 - \frac{(r-60)30}{400} \quad 60 \leq r \quad (15)$$

for the same limits of  $r$ . This bogus (referred to as V-bogus 4) assumed the same maximum wind and radius of maximum wind as V-bogus 1, but produced a significantly smaller storm, as can be seen by comparing Fig. 22 and Fig. 23. As a result of a greater vorticity maximum and the smoother, V-bogus 4 produced greater maximum winds ( $67 \text{ m s}^{-1}$ ) than V-bogus 1 ( $57 \text{ m s}^{-1}$ ). However, the greater winds did not increase the size of the storm. Because the storm was still reasonably small, boundary values closely resembled those of V-bogus 3 and the original analyzed values, whereas V-bogus 1 had created significant changes in boundary values. Resultant vorticities produced by the different bogusing techniques are plotted in Fig. 24. Note the faster decline in vorticity with increasing radius produced by V-bogus 3 (and the similar V-bogus 4).

48-hour forecasts made using V-bogus 4 and Rh-bogus 2 produced dramatic improvements in the track for Typhoon PAMELA (see Fig. 25). By 24 hours, V-bogus 4 produced 300-400% more convective precipitation and heating over the storm, but increased convection in other areas by less than 10%.

## V. CONCLUSIONS

The primitive equation model tested appeared to be very sensitive to latent heating effects produced by convection. Since the convective parameterization was initiated by the vertically integrated moisture convergence, proper representation of initial wind and moisture conditions at all levels was important. A moisture bogus consisting of a uniform field of low relative humidities with an area of higher relative humidities centered over the storm enhanced development of the storm while suppressing convection and development in areas not associated with the storm. The model also demonstrated some sensitivity to small changes in the initial values used in the moisture bogus.

Experiments conducted using the Penn State model and another primitive equation model in conjunction with a simple vorticity bogus (V-bogus 1) showed that forecast storm tracks could be improved over forecasts made using the FNWC analyzed wind fields. Premature recurvature produced in the Penn State model forecasts was retarded by using a smaller, less intense vortex (V-bogus 3). Alternatively, more recurvature was induced by increasing the maximum wind used in V-bogus 3. This bogus produced more intense winds than V-bogus 1 without introducing a large cyclonic area. The smaller more intense vortex improved



forecast tracks over V-bogus 1 and the less intense version of V-bogus 3 in the Penn State model forecasts. It was therefore possible to produce significant, and somewhat controlled, changes in the forecast tracks of individual storms by varying the size and intensity of the initial bogus.

Future experiments should include increased resolution of the horizontal domain. The SSI model appeared to have an advantage in representing steering currents because of its finer resolution. The initial wind maximum introduced by the bogus could not be sustained on the 120 km grid, and marked reductions in intensities occurred for all boguses used. Given finer resolution, V-bogus 3 using a variable maximum wind based on observations of the storm should provide a well-structured storm which does not get too large.

The development of strong shears and convergence which produced convection along the boundaries, indicated that modifications to the boundary conditions should also be considered in future experiments. Changes to the model which could resolve these effects are the inclusion of moisture diffusion and the addition of large-scale changes close to the boundaries. One possibility is the use of a scheme described by Perkey and Kreitzberg (1976) where a fraction of the large-scale time change (based either on analyses or from forecasts produced by a large-scale model) is added to

the model predicted tendency depending on the proximity  
to the boundary.

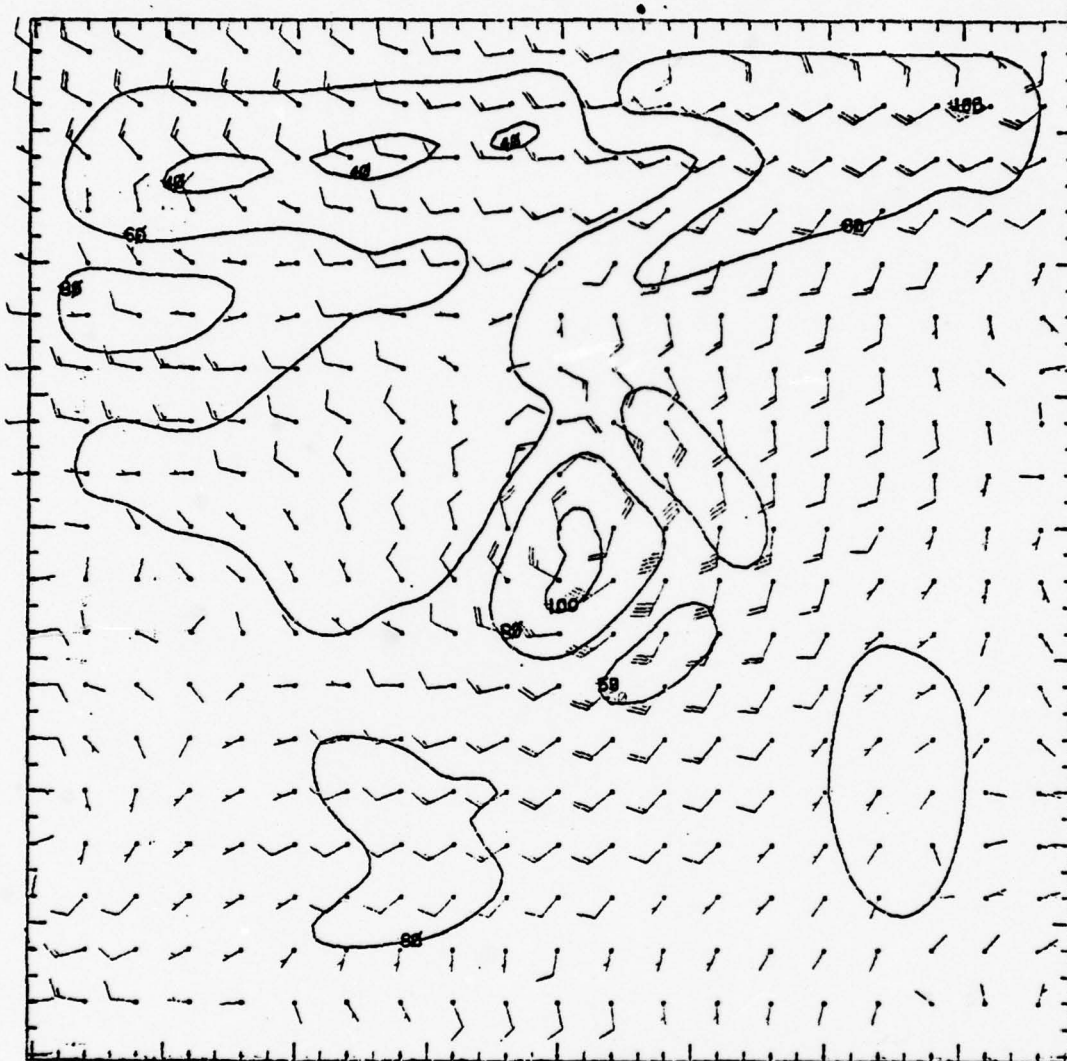


Figure 1. Typhoon KIM 24-h forecast VT 77111012  
 600 mb winds ( $\text{m s}^{-1}$ ) and relative  
 humidity (coordinates are grid points  
 vice latitude and longitude)

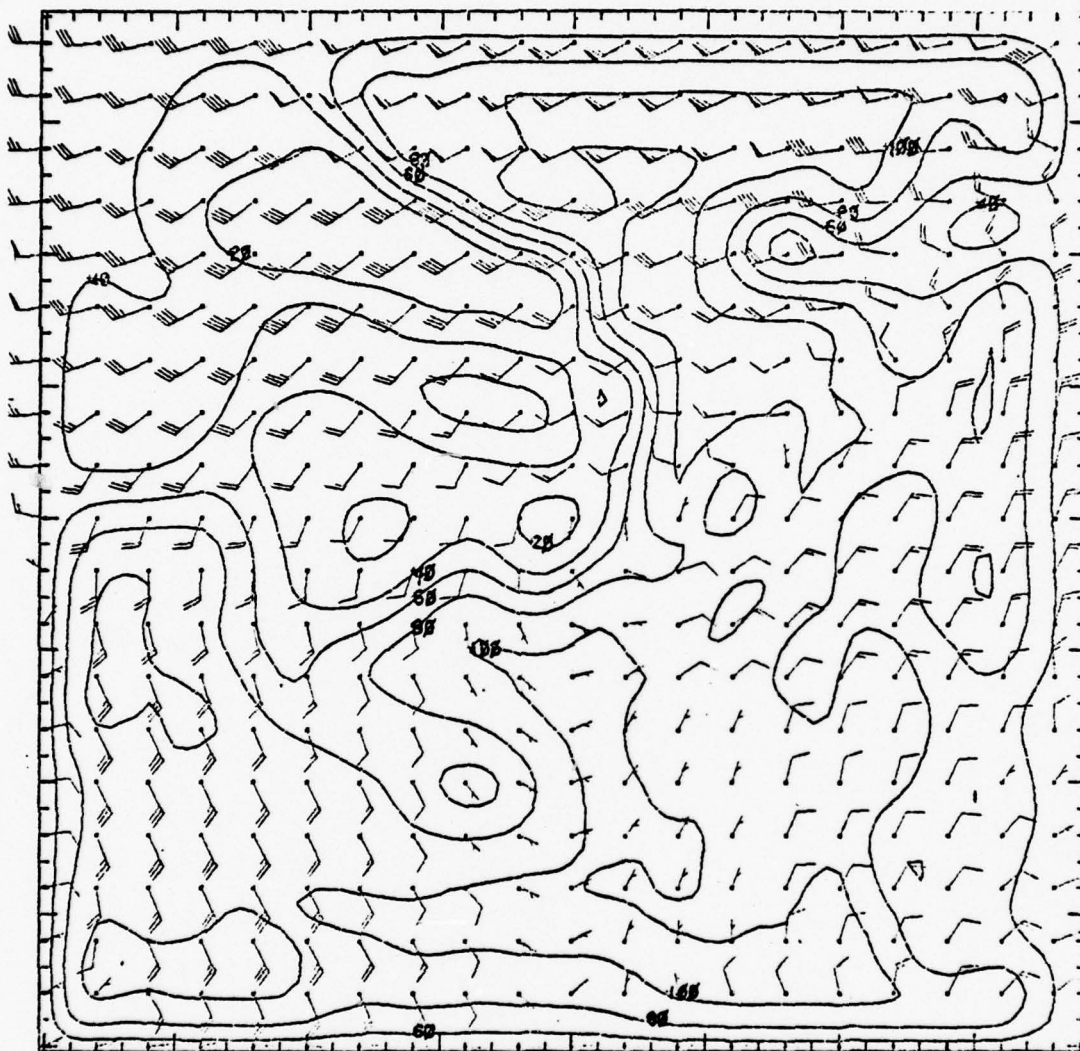


Figure 2. Typhoon KIM 48-h forecast VT 77111112  
150 mb winds ( $\text{m s}^{-1}$ ) and relative  
humidity (isoline spacing is 20%)



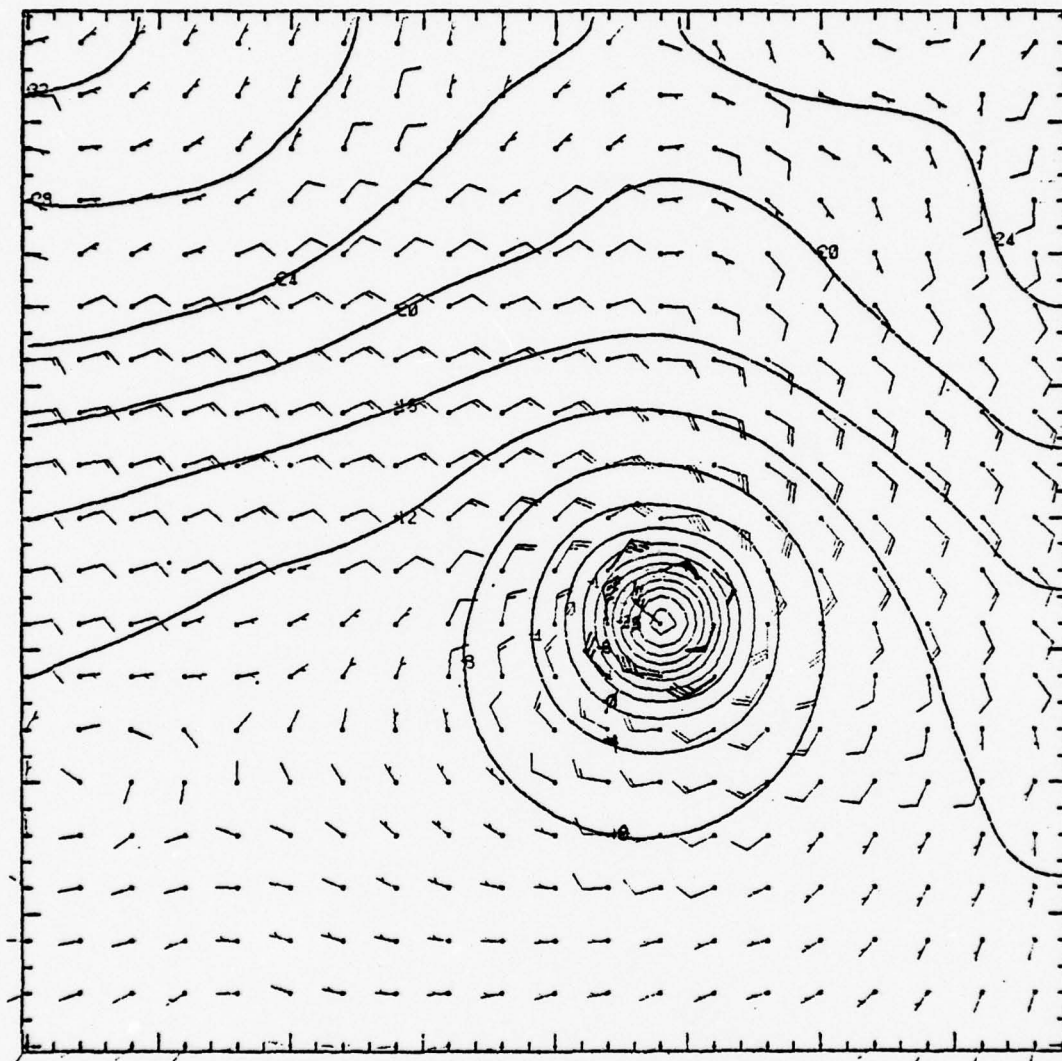


Figure 3a. Typhoon KIM initial field SLP-1000 mb and winds ( $\text{m s}^{-1}$ ) at  $\sigma = .95$  using V-bogus 1 (isoline spacing is 4 mb)

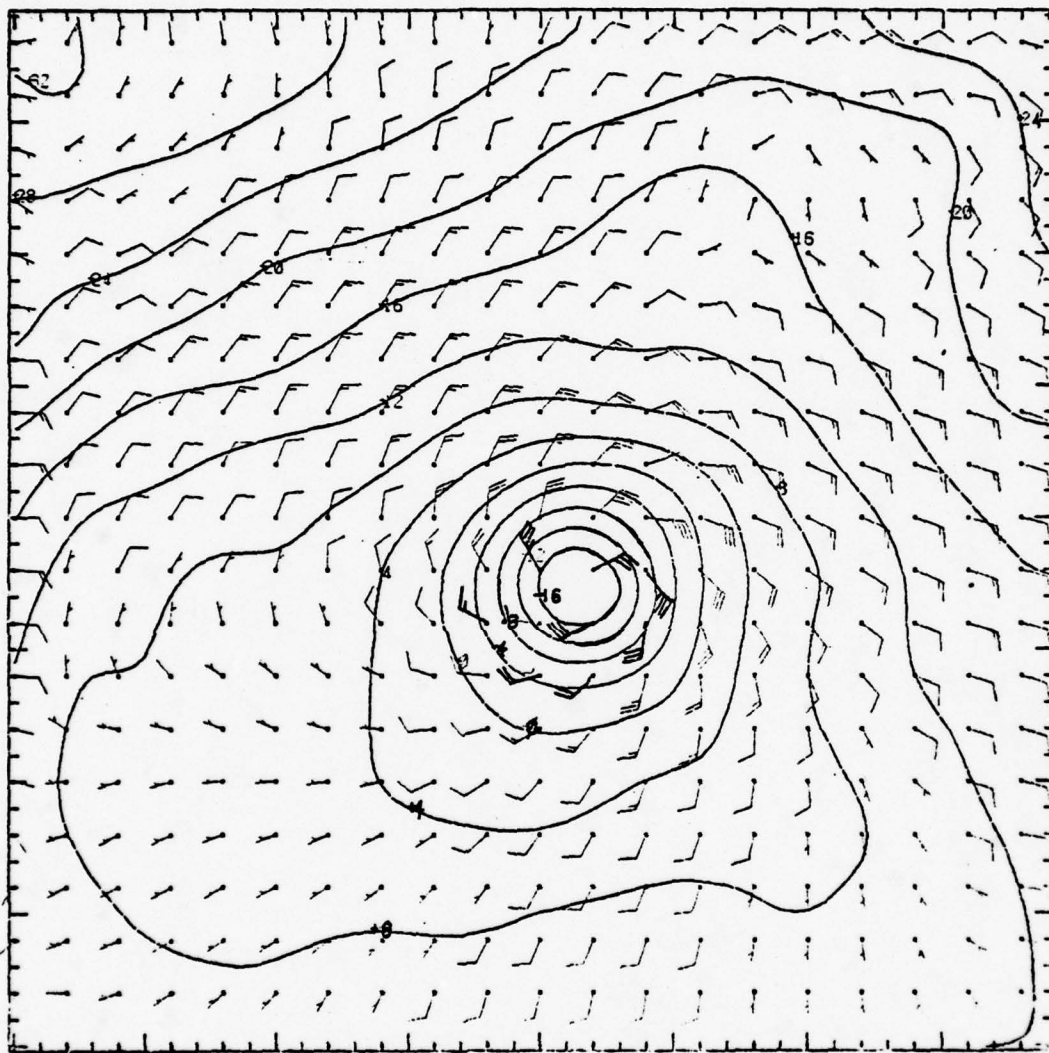


Figure 3b. Typhoon KIM 12-h forecast SLP-1000 mb and winds ( $\text{m s}^{-1}$ ) at  $\sigma = .95$  using V-bogus 1 and Rh-bogus 1

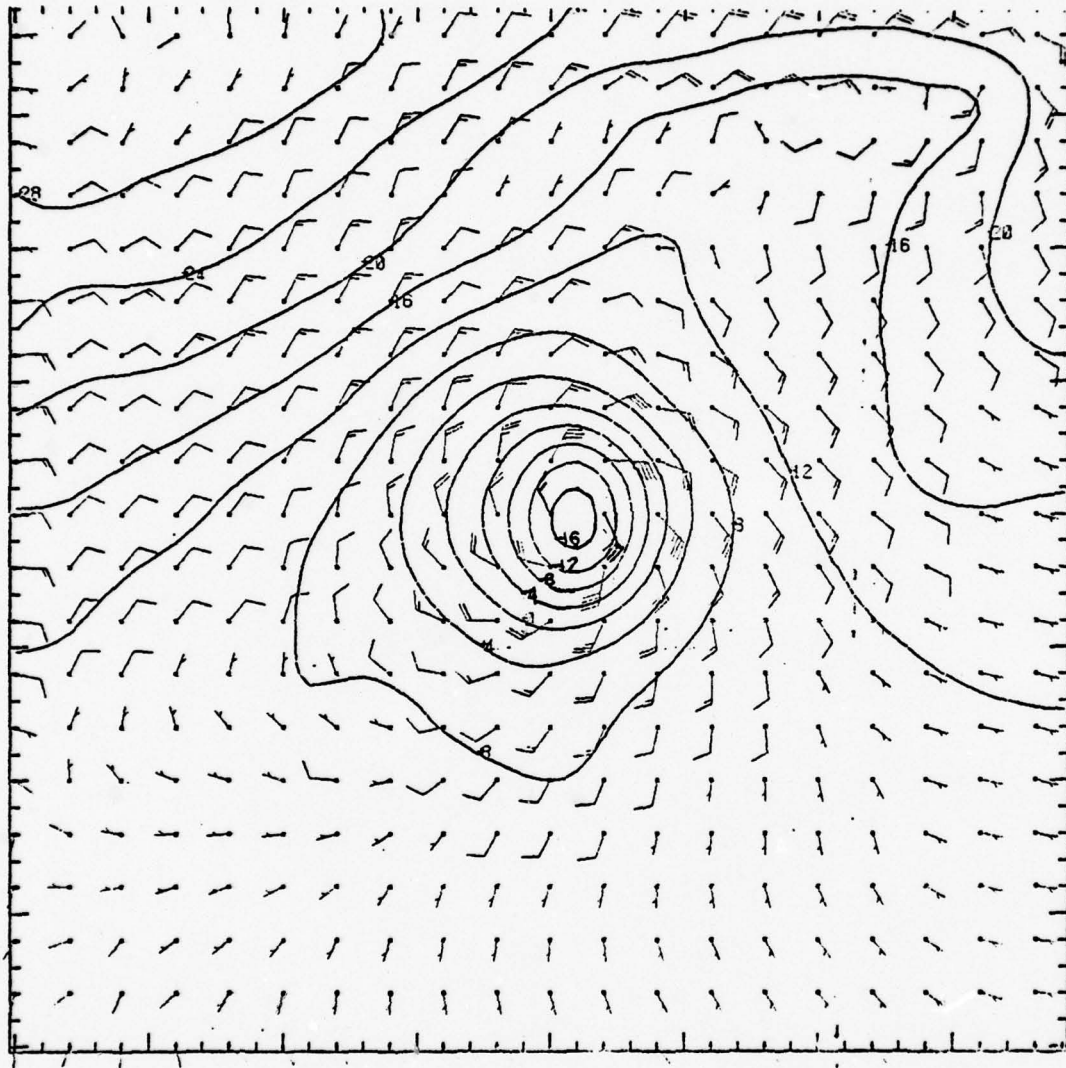


Figure 3c. Typhoon KIM 24-h forecast SLP-1000 mb and winds ( $\text{m s}^{-1}$ ) at  $\sigma = .95$  using V-bogus 1 and Rh-bogus 1

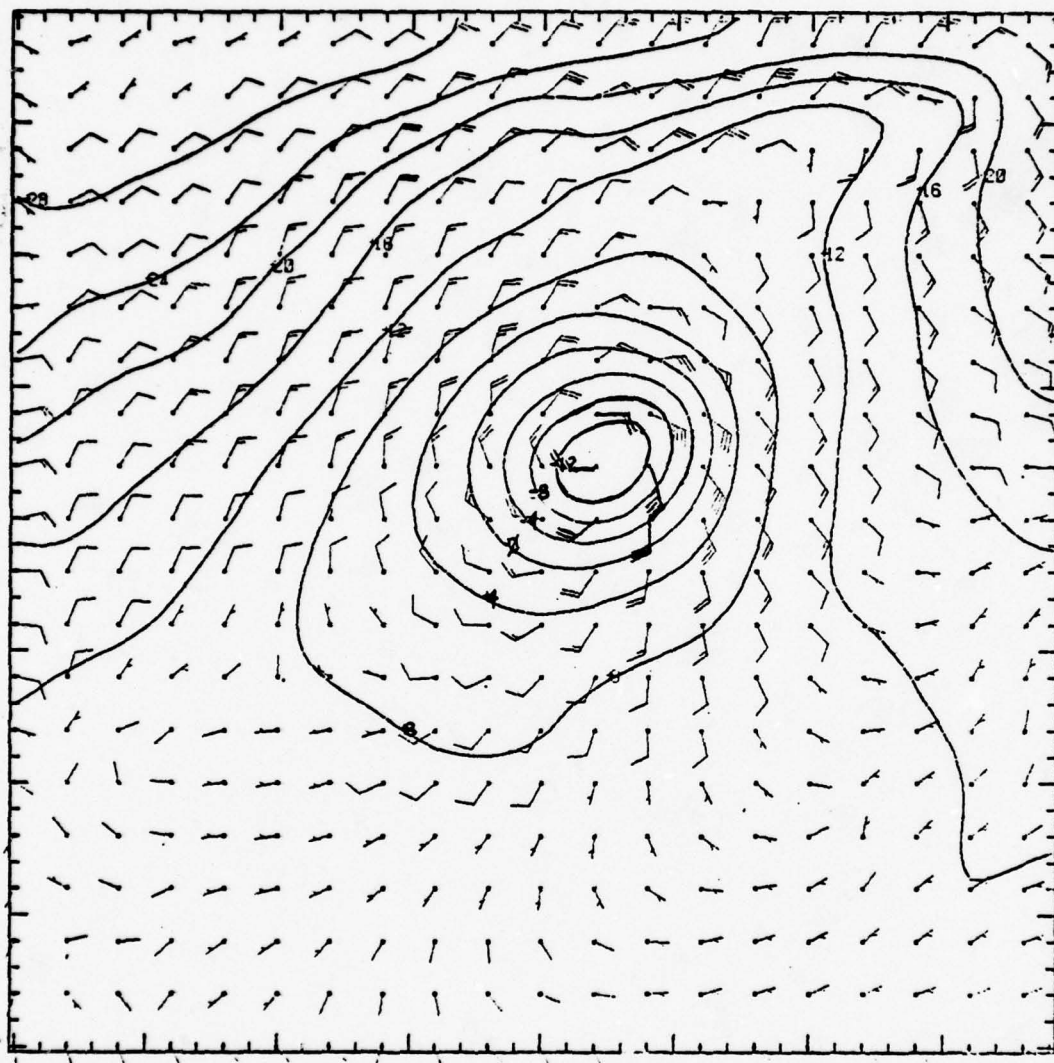


Figure 3d. Typhoon KIM 36-h forecast SLP-1000 mb  
and winds ( $\text{m s}^{-1}$ ) at  $\sigma = .95$  using  
V-bogus 1 and Rh-bogus 1



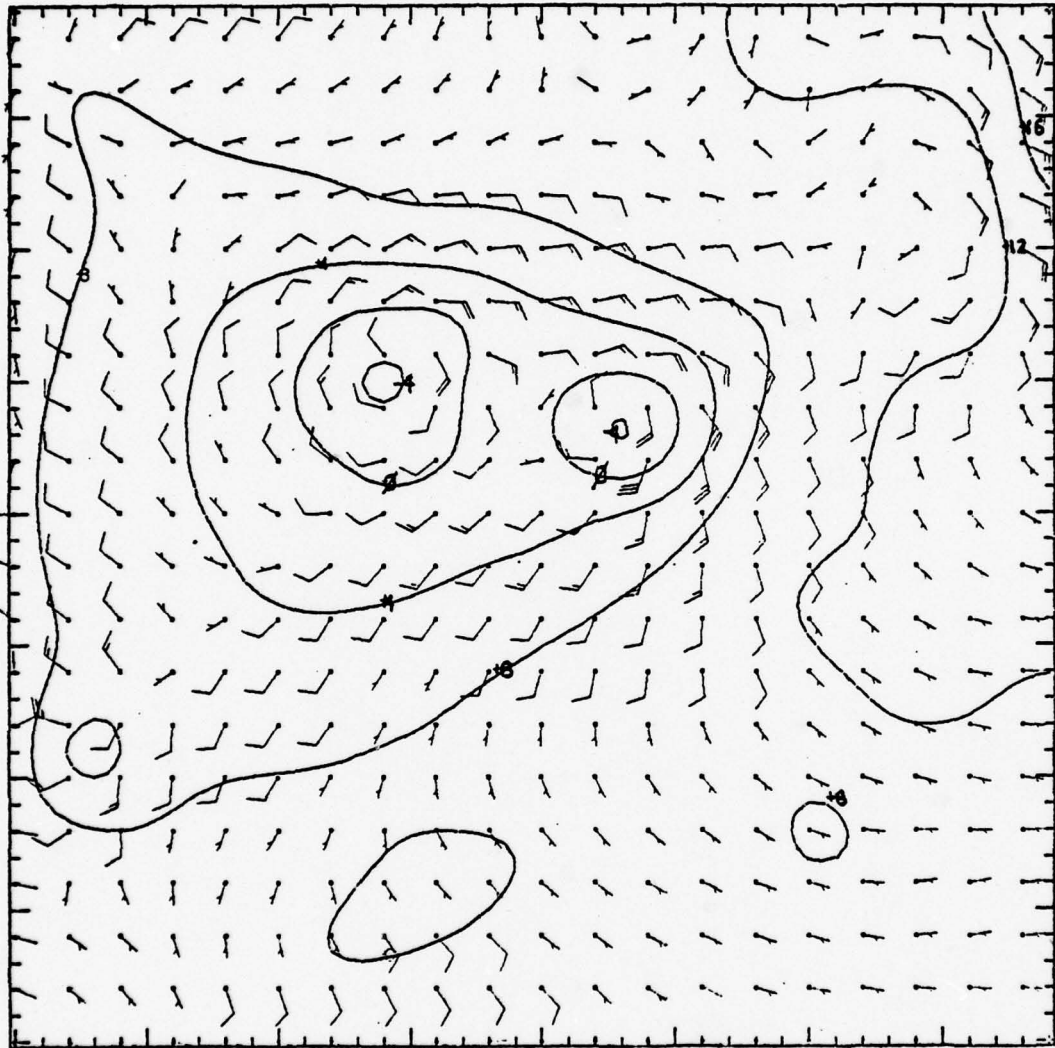


Figure 4. Typhoon OLIVE 36-h forecast VT 78042300  
SLP-1000 mb and winds ( $\text{m s}^{-1}$ ) at  $\sigma = .95$   
using V-bogus 1 and Rh-bogus 1



Figure 5. Typhoon OLIVE 36-h forecast VT 78042300  
accumulated convective precipitation  
(cm) using V-bogus 1 and Rh-bogus 1.  
Center value of Olive is 20 cm (isoline  
spacing is 1 cm)

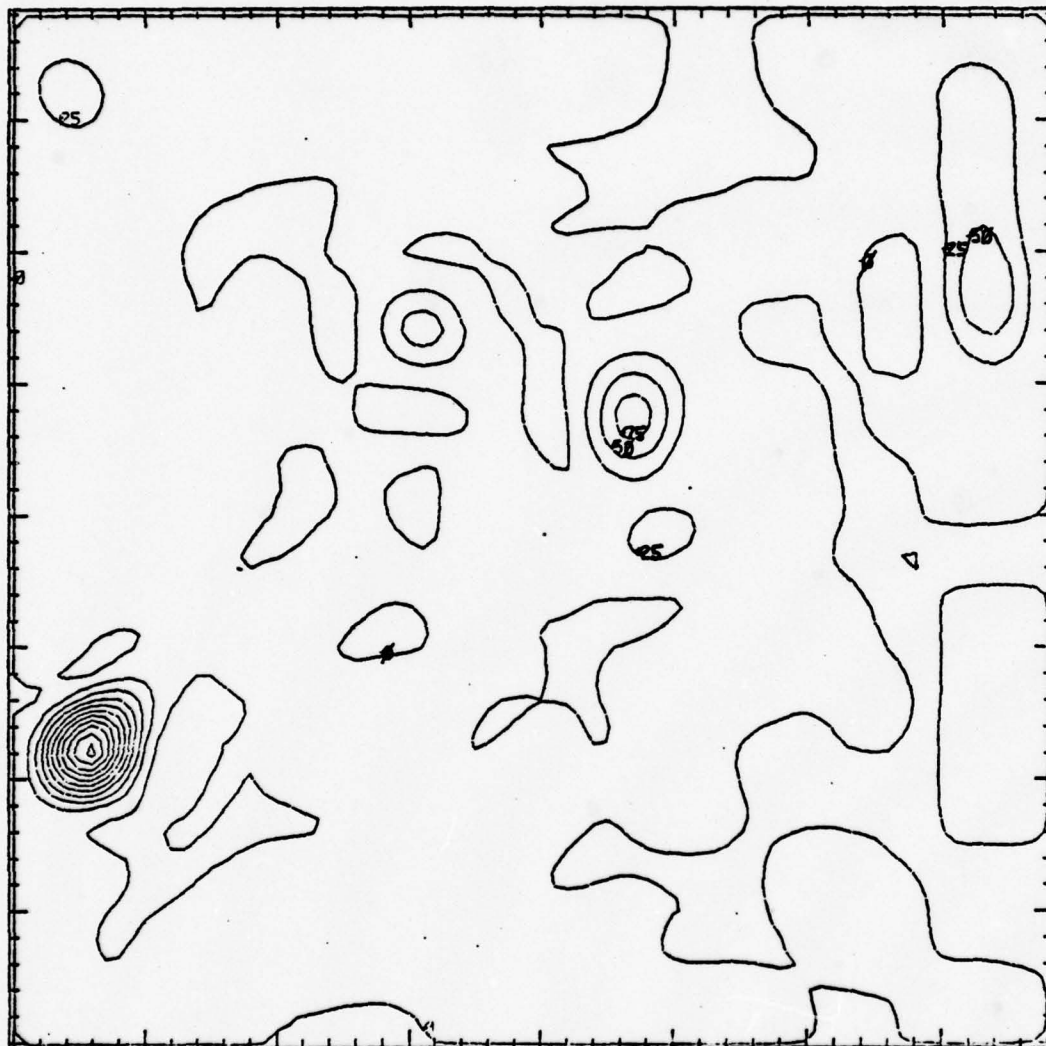


Figure 6. Typhoon OLIVE 36-h forecast VT 78042300  
convective heating ( $^{\circ}\text{C}/\text{day}$ ) using  
V-bogus 1 and Rh-bogus 1 (isoline  
spacing is  $25\text{ }^{\circ}\text{C}/\text{day}$ )

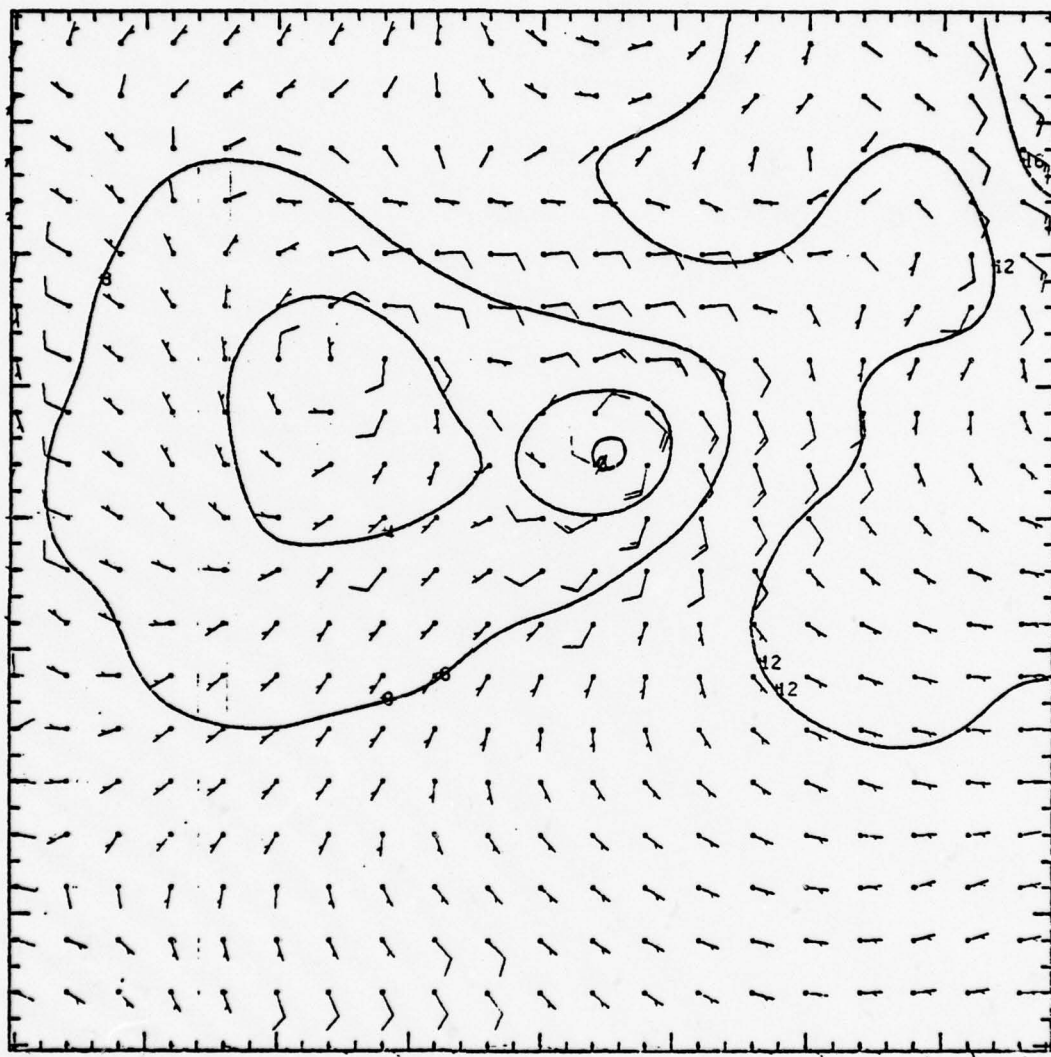


Figure 7. Typhoon OLIVE 36-h forecast VT 78042300  
 SLP-1000 mb and winds ( $\text{m s}^{-1}$ ) at  
 $\sigma = .95$  using V-bogus 1 and Rh-bogus 2



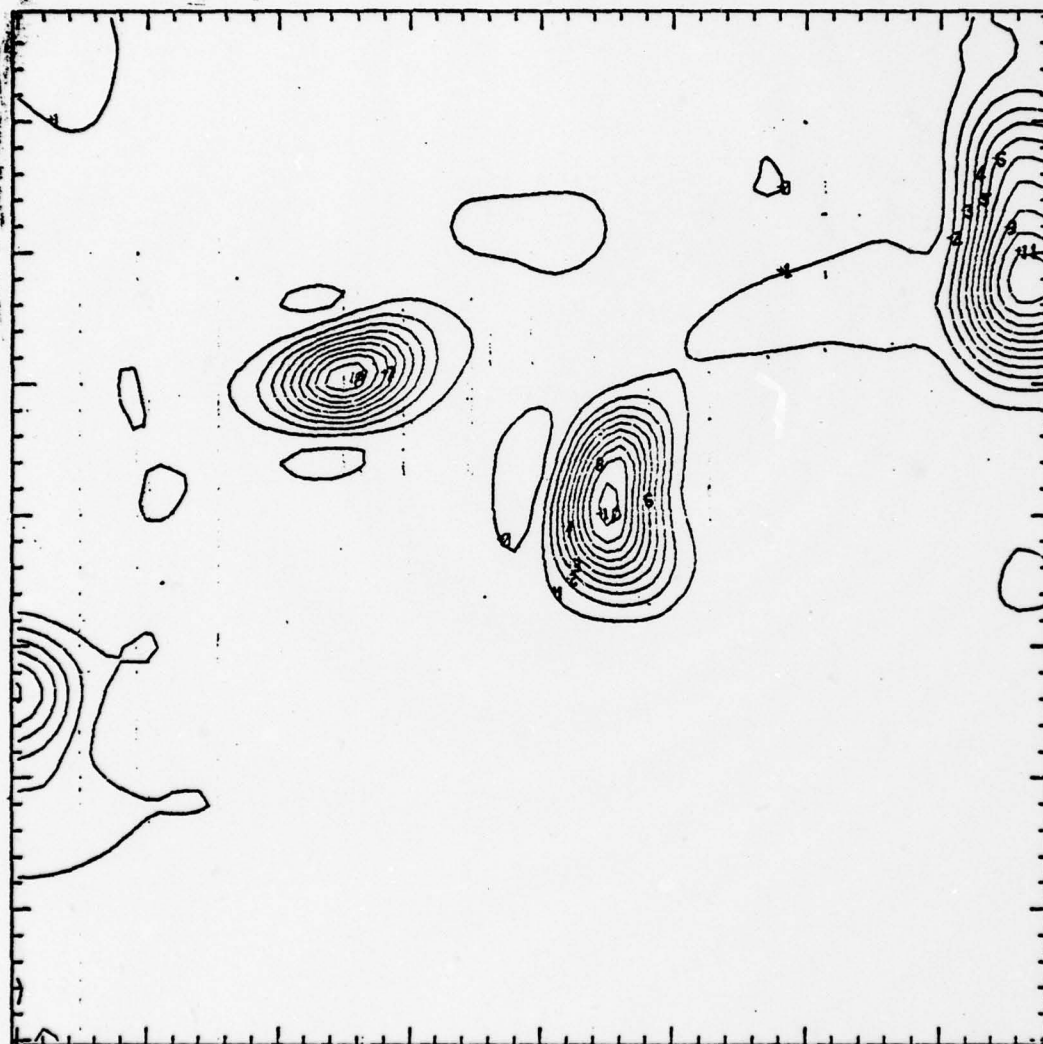


Figure 8. Typhoon OLIVE 36-h forecast VT 78042300  
accumulated convective precipitation (cm)  
using V-bogus 1 and Rh-bogus 2

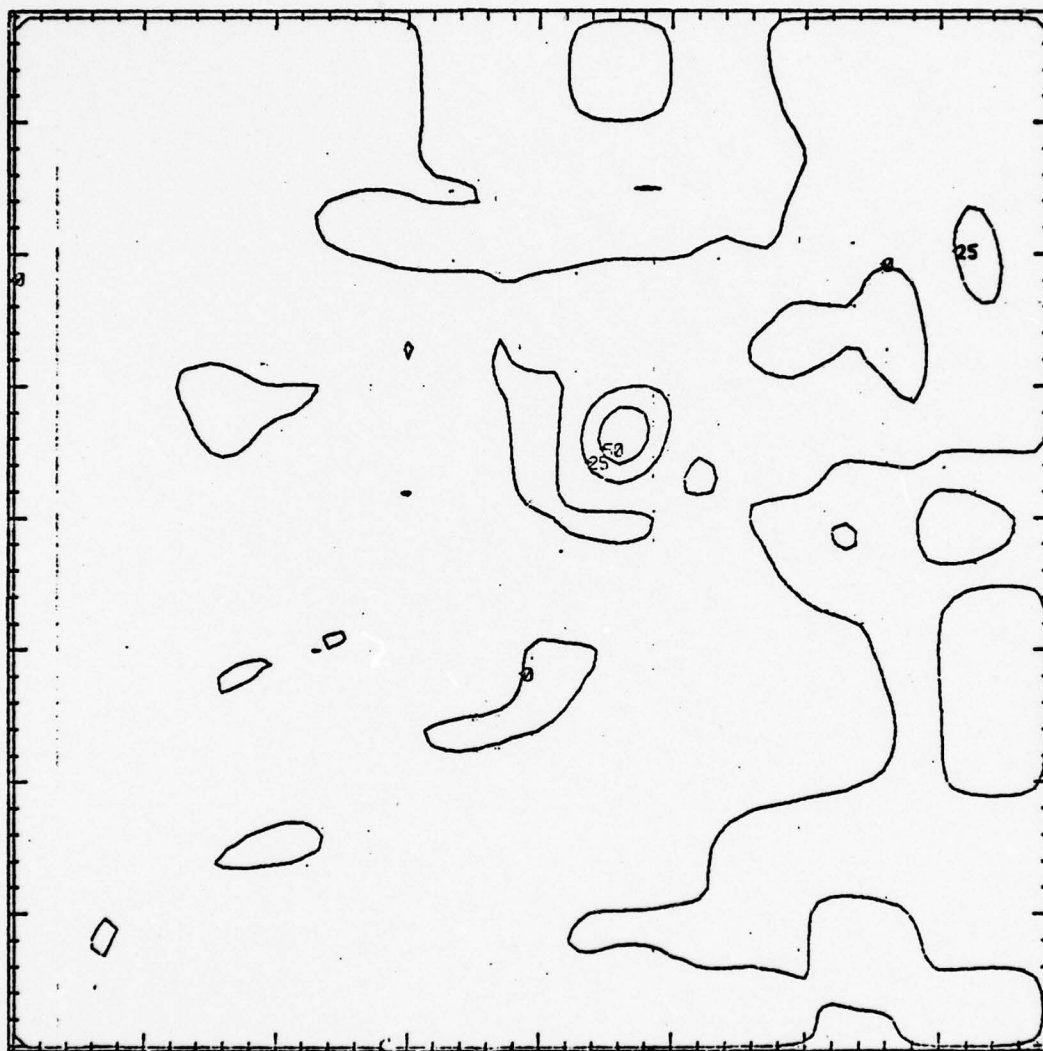


Figure 9. Typhoon OLIVE 36-h forecast VT 78042300  
convective heating ( $^{\circ}\text{C}/\text{day}$ ) using  
V-bogus 1 and Rh-bogus 2

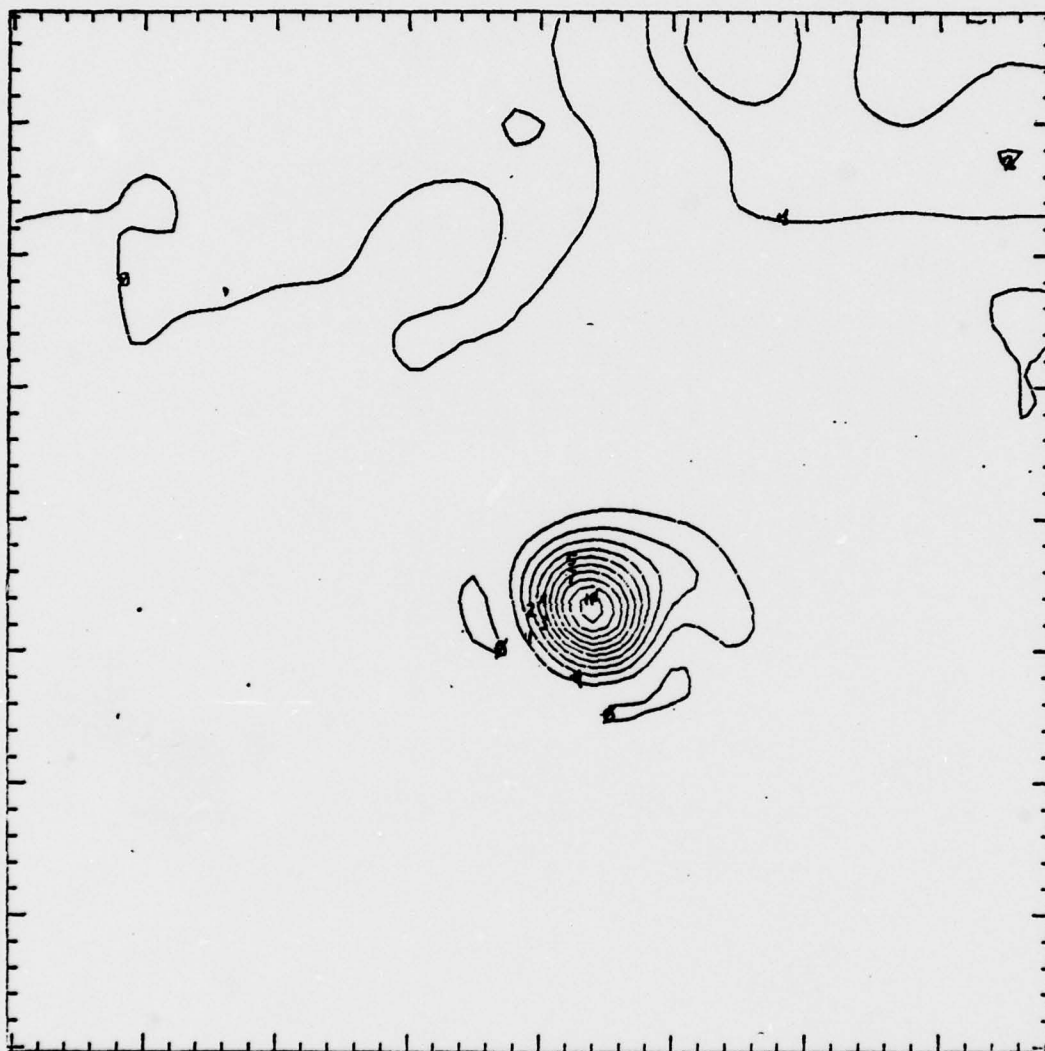


Figure 10a. Typhoon KIM 12-h forecast VT 77111000  
accumulated convective precipitation (cm)  
using V-bogus 1 and Rh-bogus 1 before  
making changes to model constants (see text)

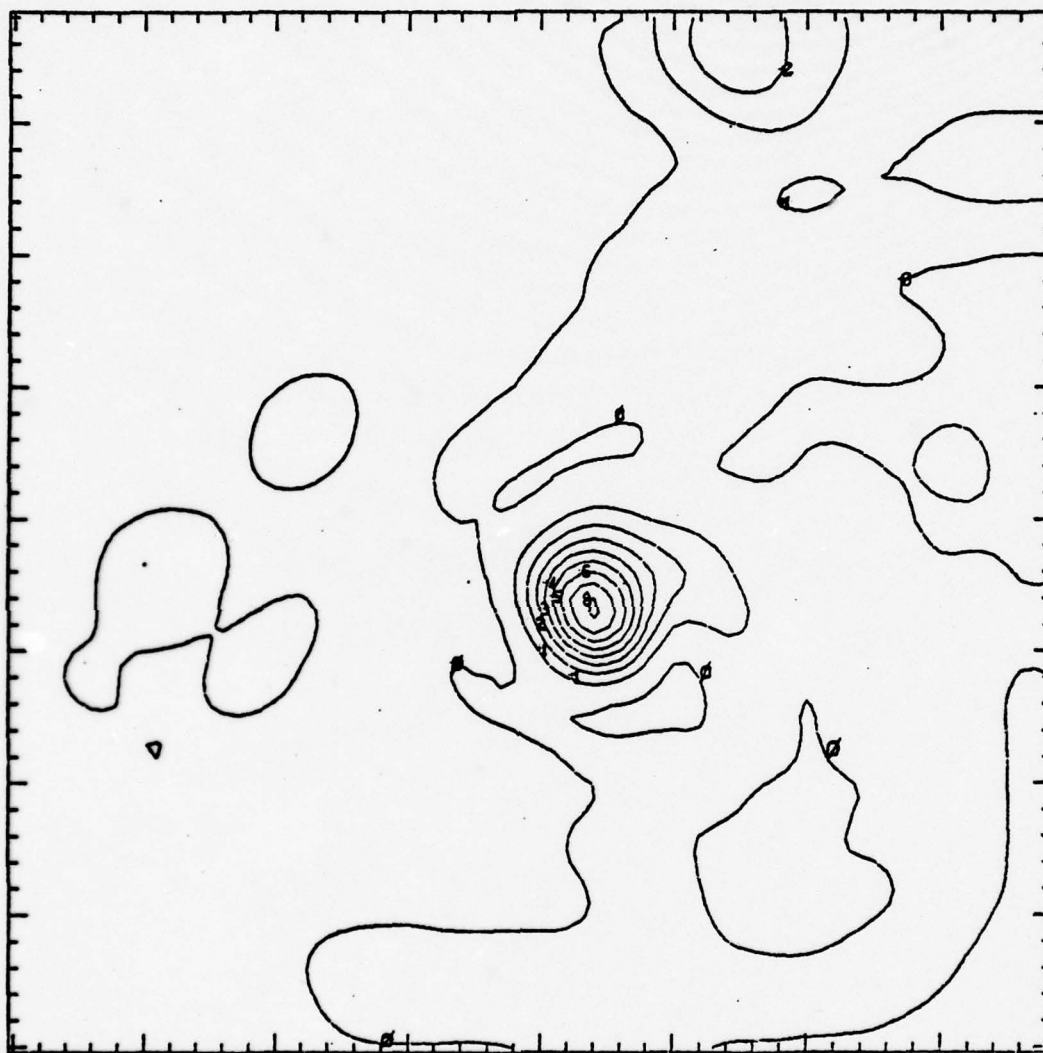


Figure 10b. Typhoon KIM 12-h forecast VT 77111000  
accumulated convective precipitation (cm)  
using V-bogus 1 and Rh-bogus 1 after  
changes to model constants (see text)



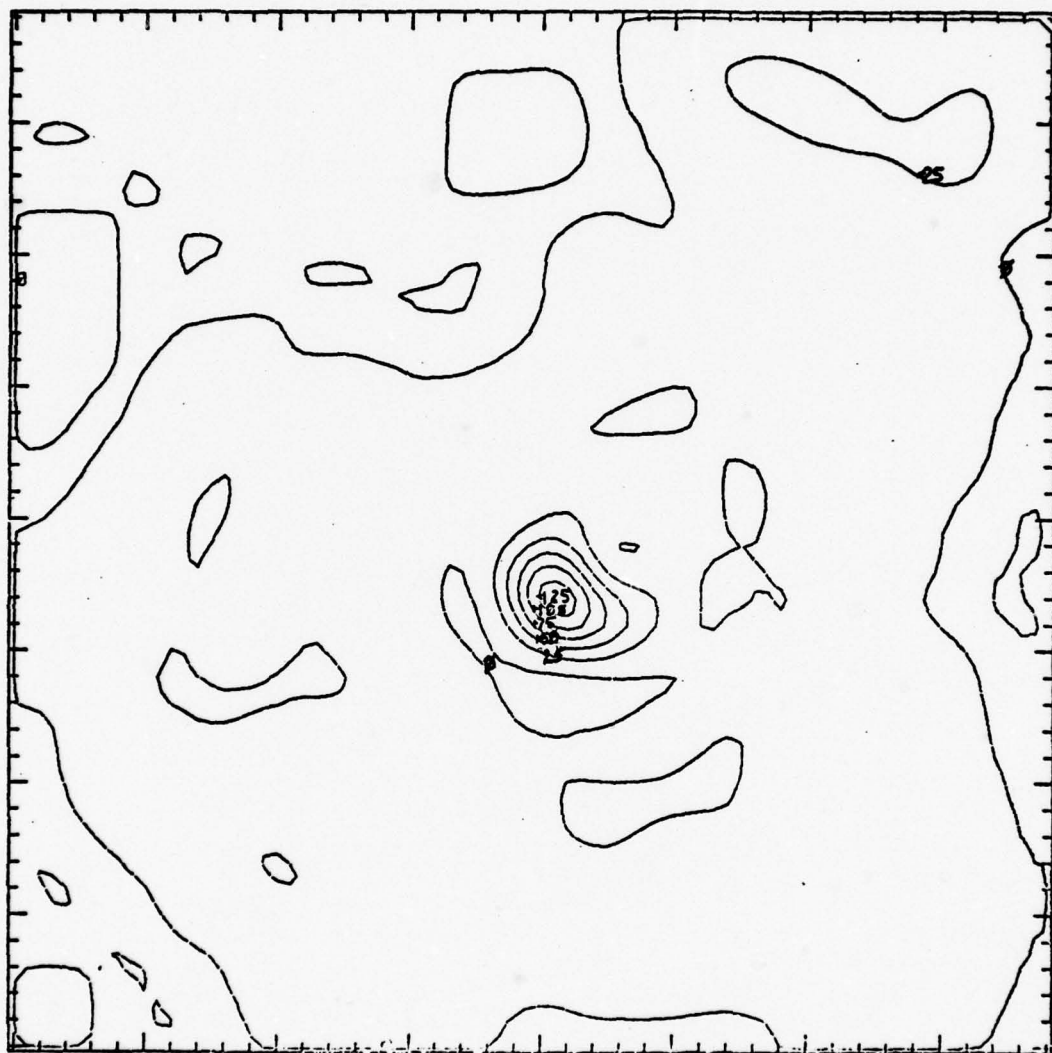


Figure 10c. Typhoon KIM 12-h forecast VT 77111000  
convective heating ( $^{\circ}\text{C}/\text{day}$ ) before  
changes to model constants (see text)

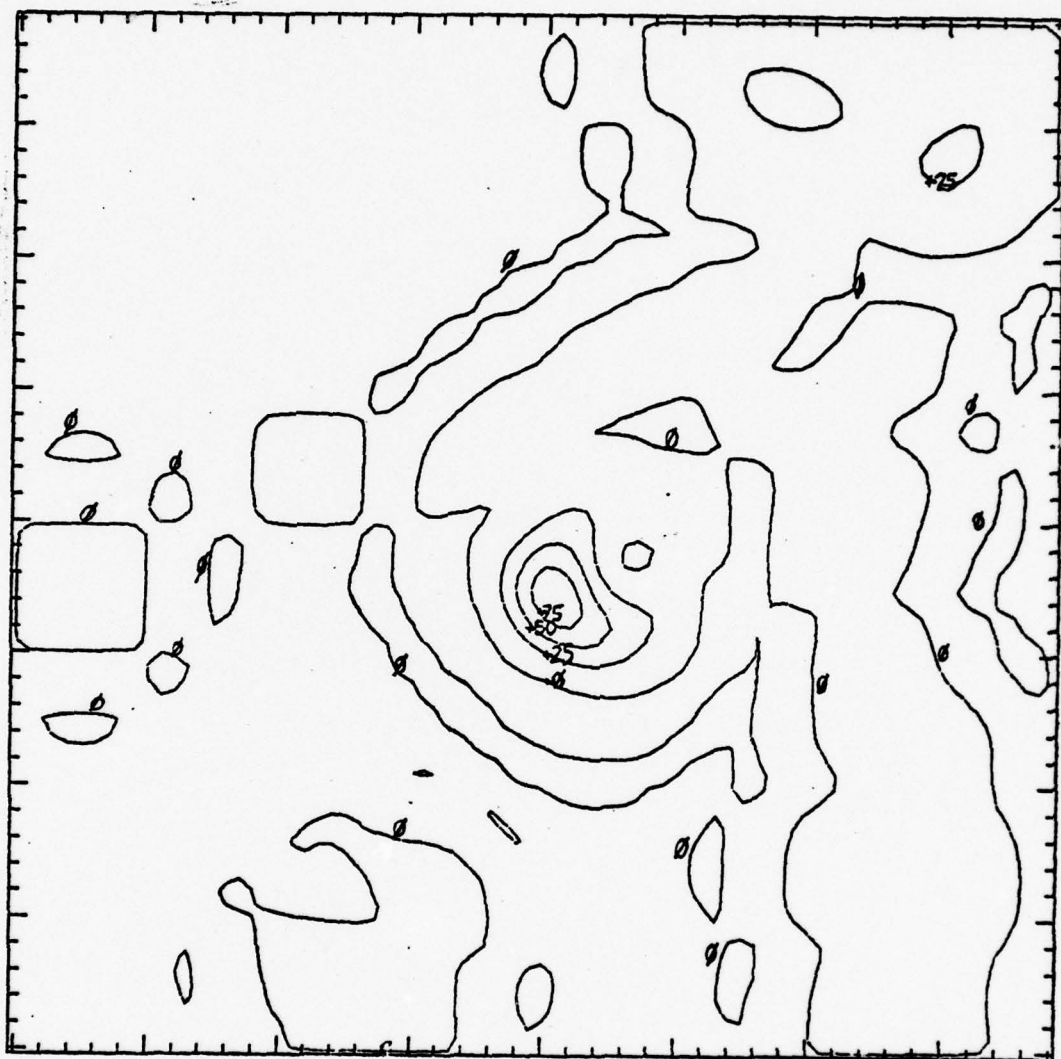


Figure 10d. Typhoon KIM 12-h forecast VT 77111000  
convective heating ( $^{\circ}\text{C}/\text{day}$ ) using  
V-bogus 1 and Rh-bogus 1 after changes  
to model constants (see text)

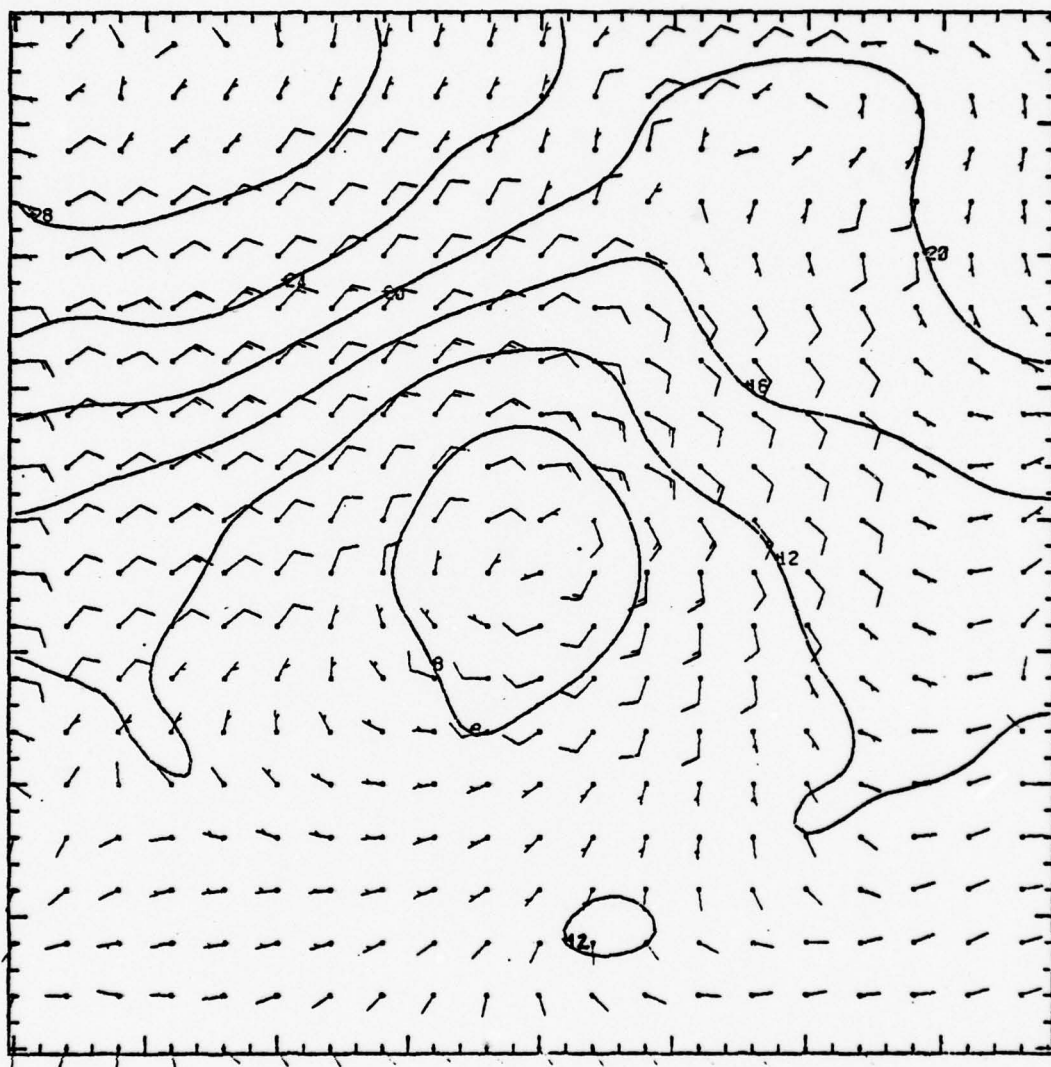


Figure 11. Typhoon KIM 24-h forecast VT 77111012  
SLP-1000 mb and winds ( $\text{m s}^{-1}$ ) at  
 $\sigma = .95$  without convective heating effects

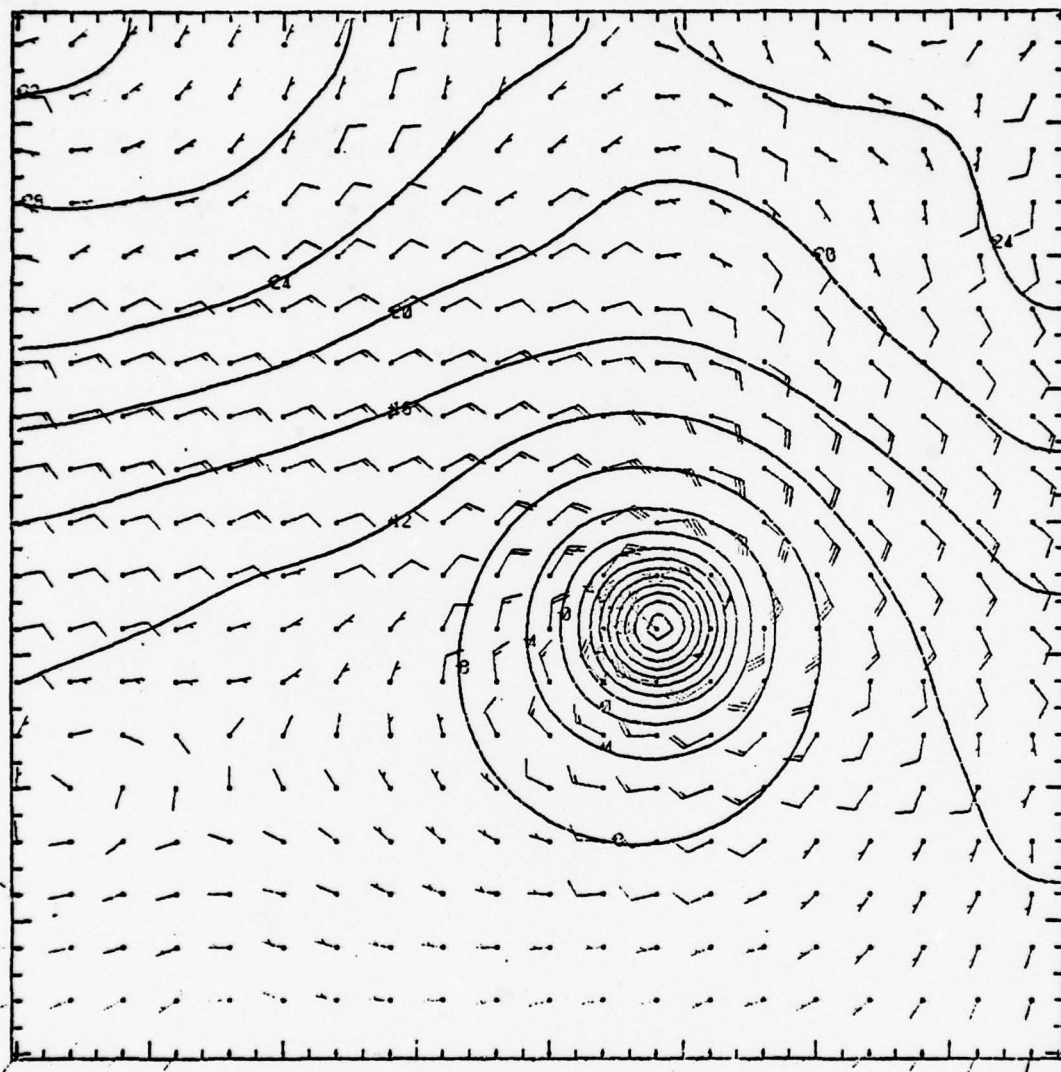


Figure 12a. Typhoon KIM initial SLP-1000 mb and winds ( $\text{m s}^{-1}$ ) at  $\sigma = .95$  using V-bogus 1



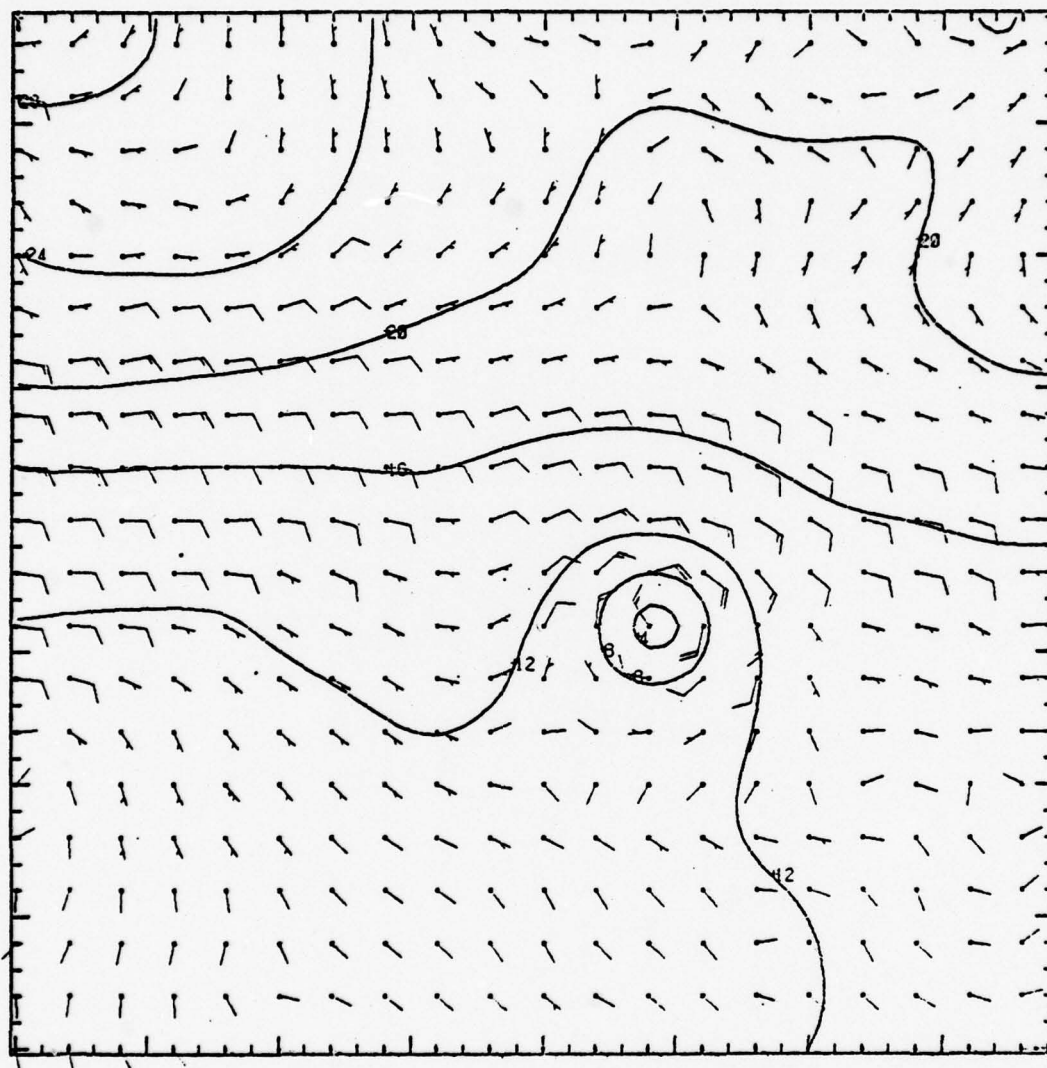


Figure 12b. Typhoon KIM<sub>1</sub> initial SLP-1000 mb and winds ( $\text{m s}^{-1}$ ) at  $\sigma = .95$  using V-bogus 3

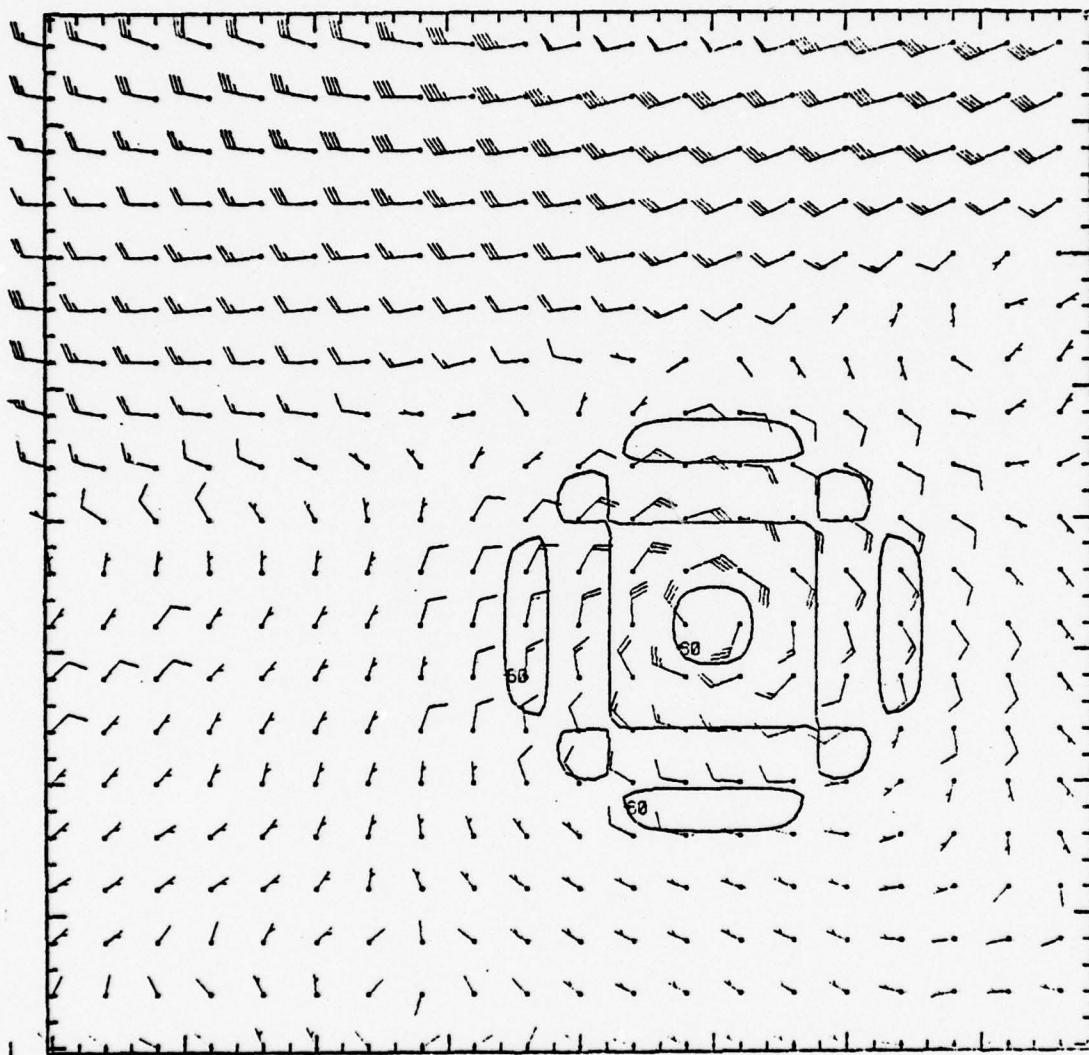


Figure 12c. Typhoon KIM initial winds ( $\text{m s}^{-1}$ ) at 400 mb using V-bogus 1, and relative humidity (Rh-bogus 1)

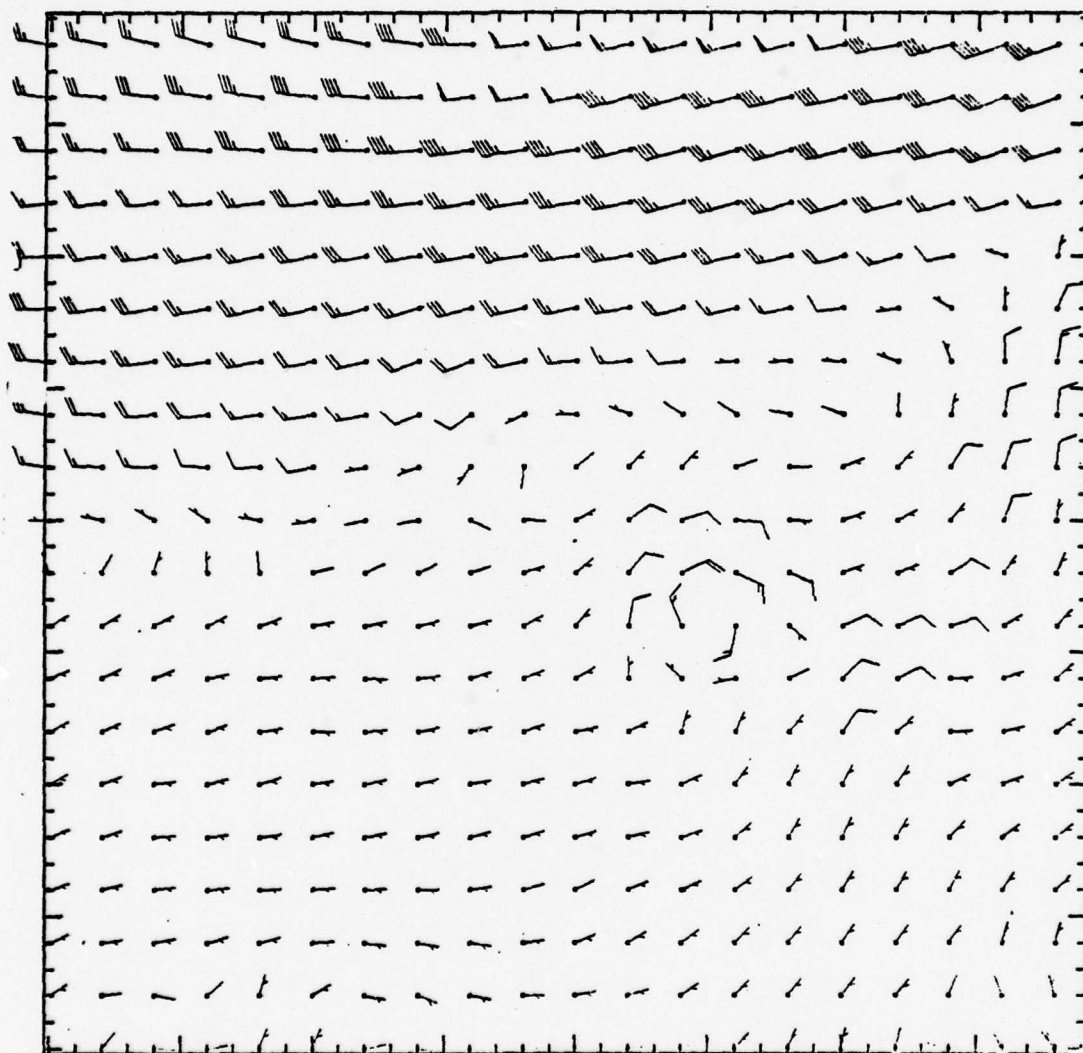


Figure 12d. Typhoon KIM initial winds ( $\text{m s}^{-1}$ )  
at 400 mb using V-bogus 3

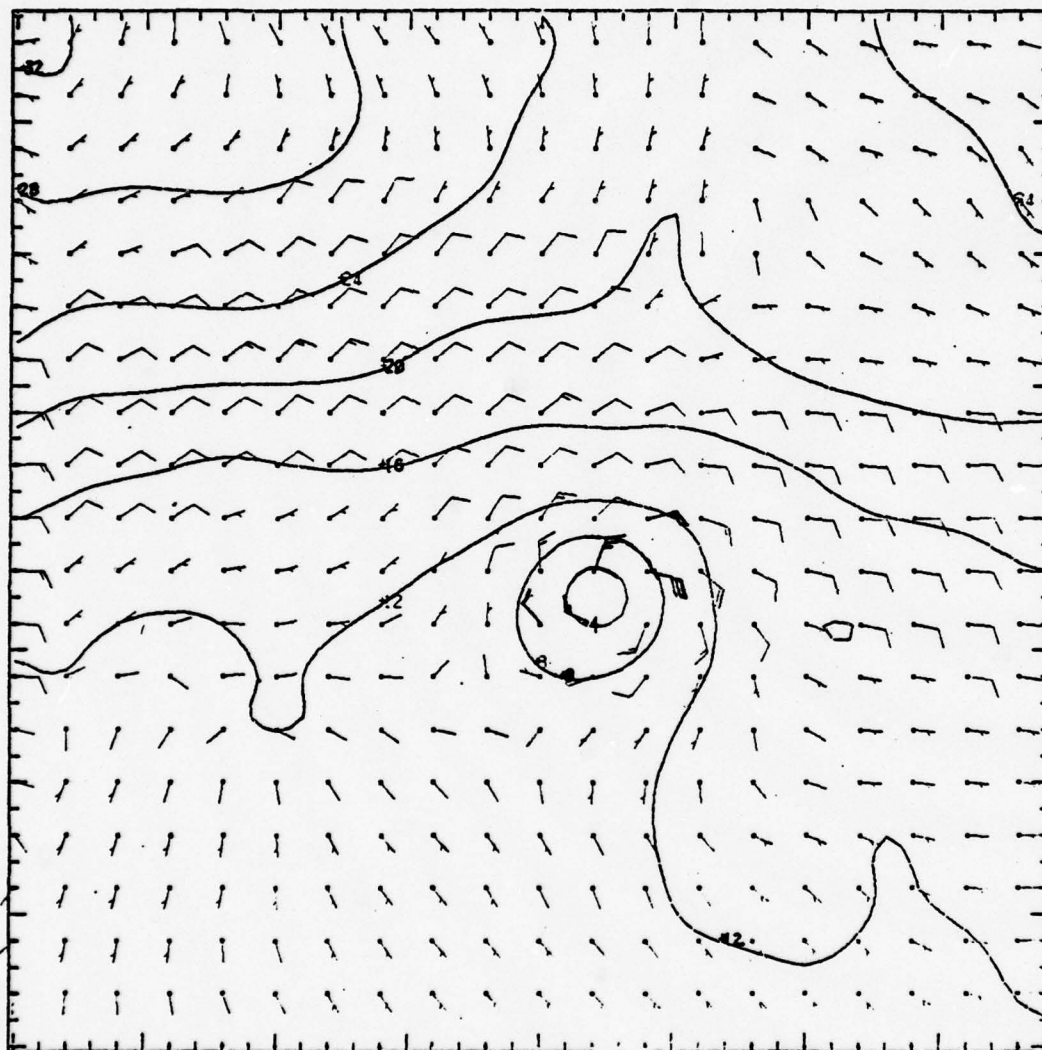


Figure 13. Typhoon KIM 12-h forecast VT 77111000  
SLP-1000 mb and winds at  $\sigma = .95$  using  
V-bogus 3 and Rh-bogus 2



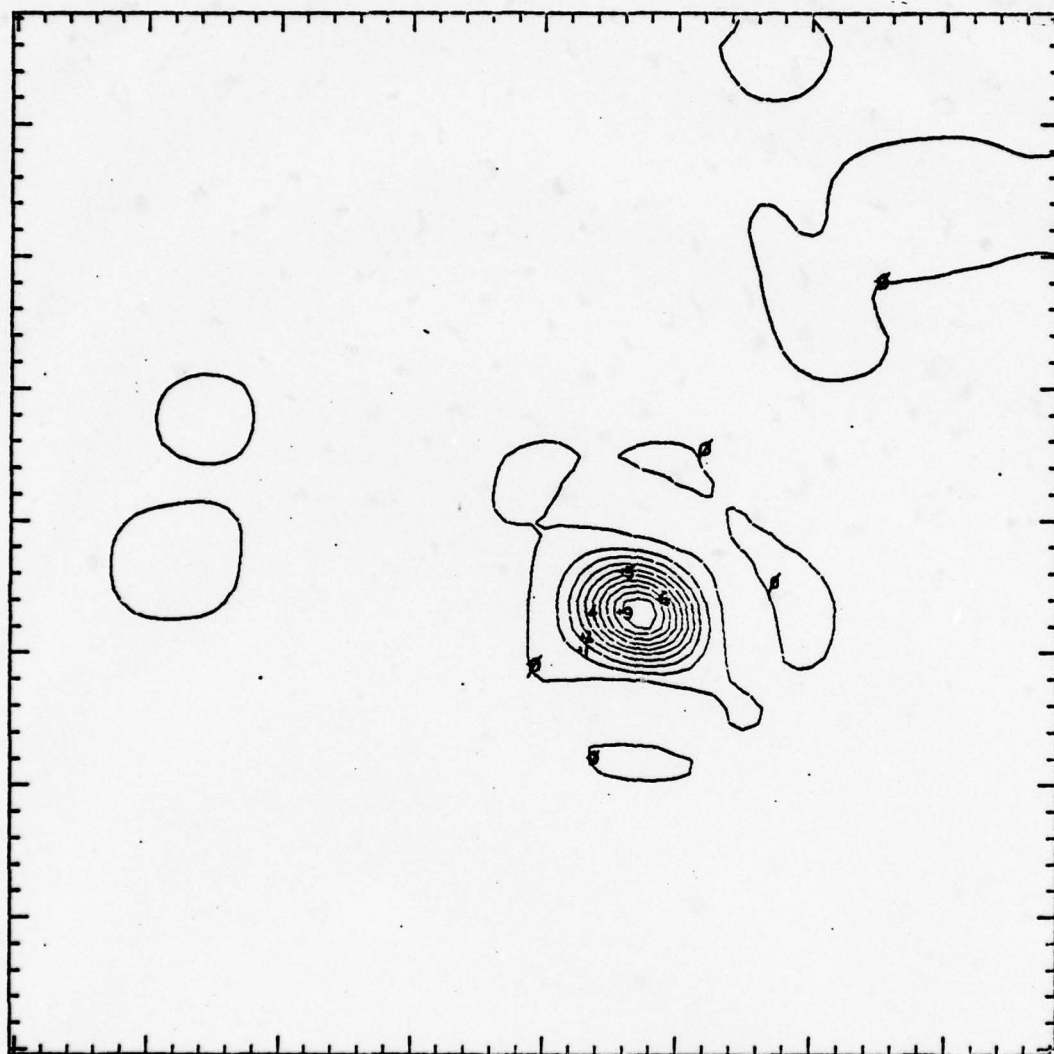


Figure 14. Typhoon KIM 12-h forecast VT 77111000  
accumulated convective precipitation  
(cm) using V-bogus 3 and Rh-bogus 2

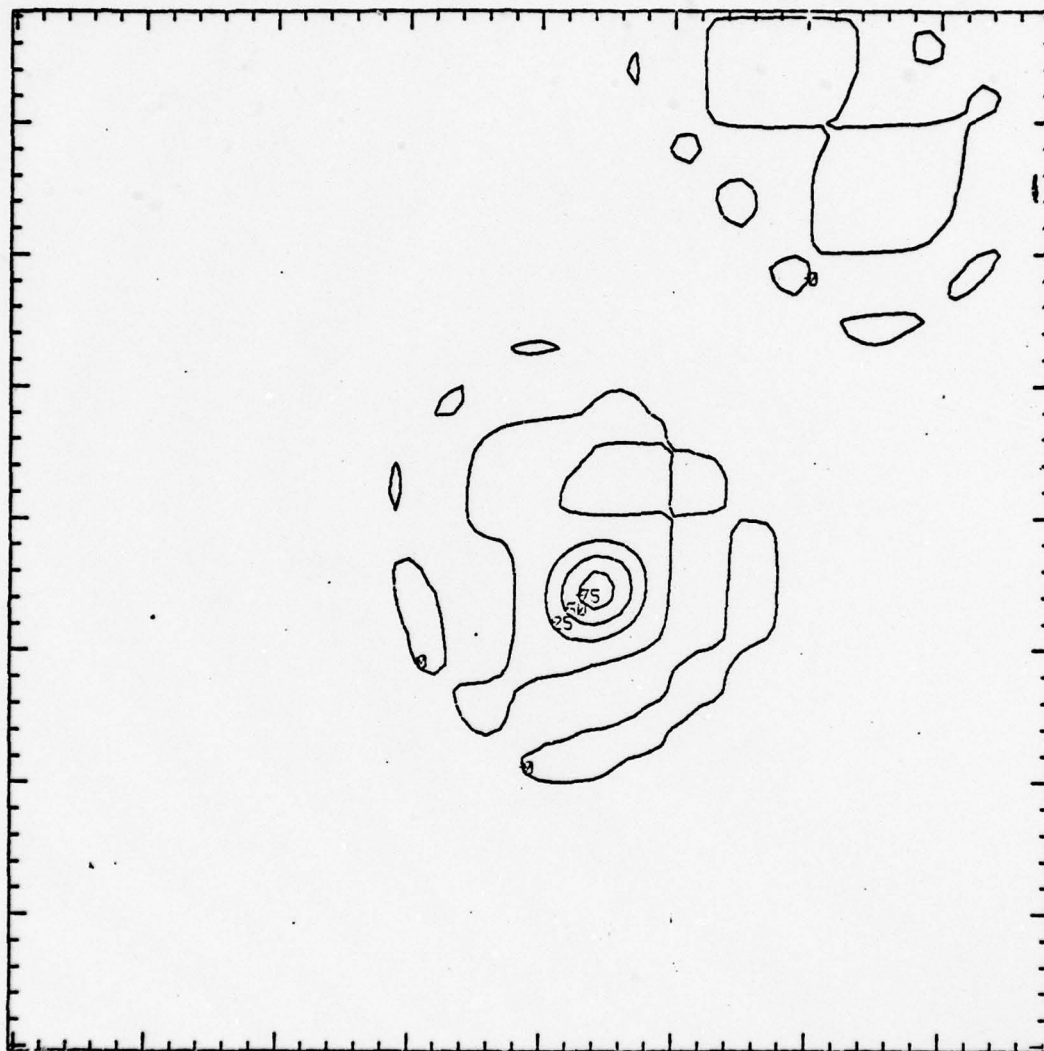


Figure 15. Typhoon KIM 12-h forecast VT 77111000  
convective heating ( $^{\circ}\text{C}/\text{day}$ ) using  
V-bogus 3 and Rh-bogus 2

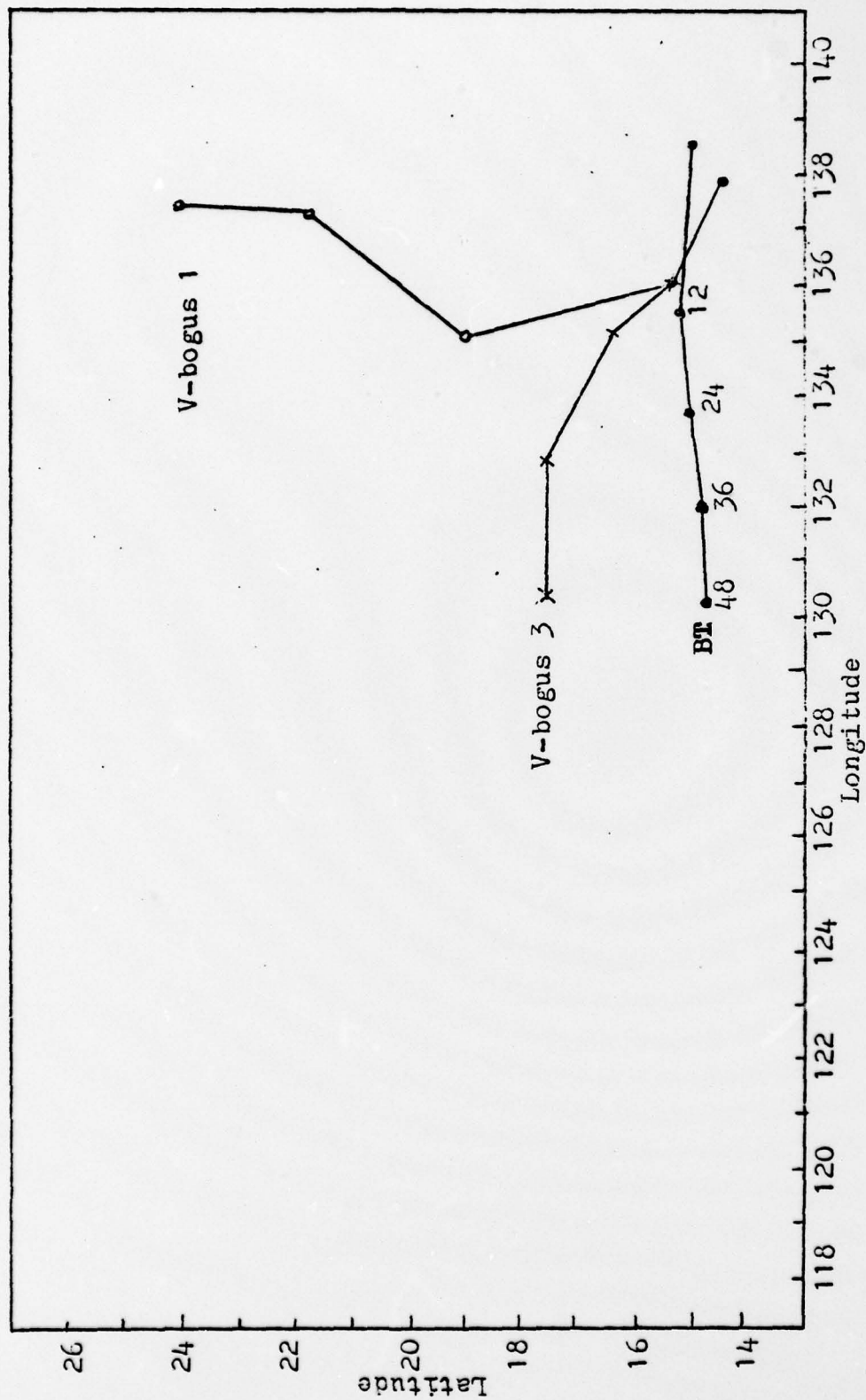


Fig. 16. Forecast tracks of Typhoon KIM(77110912) for V-bogus 1 vs V-bogus 2 in the Penn State model.

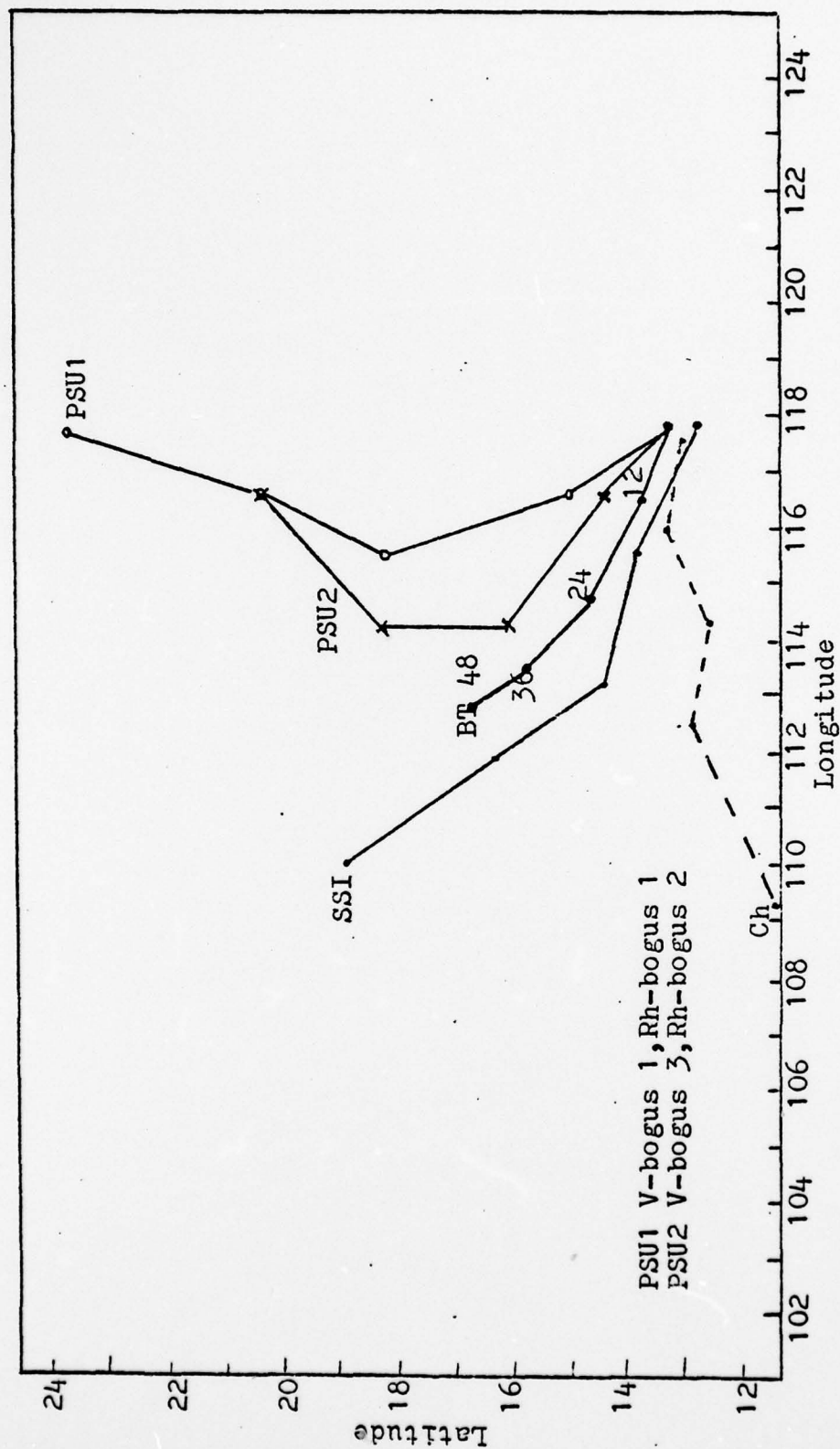


Fig. 17. Forecast tracks of Typhoon OLIVE(78042112) using the Penn State(PSU), split semi-implicit (SSI), and Channel(Ch) models.



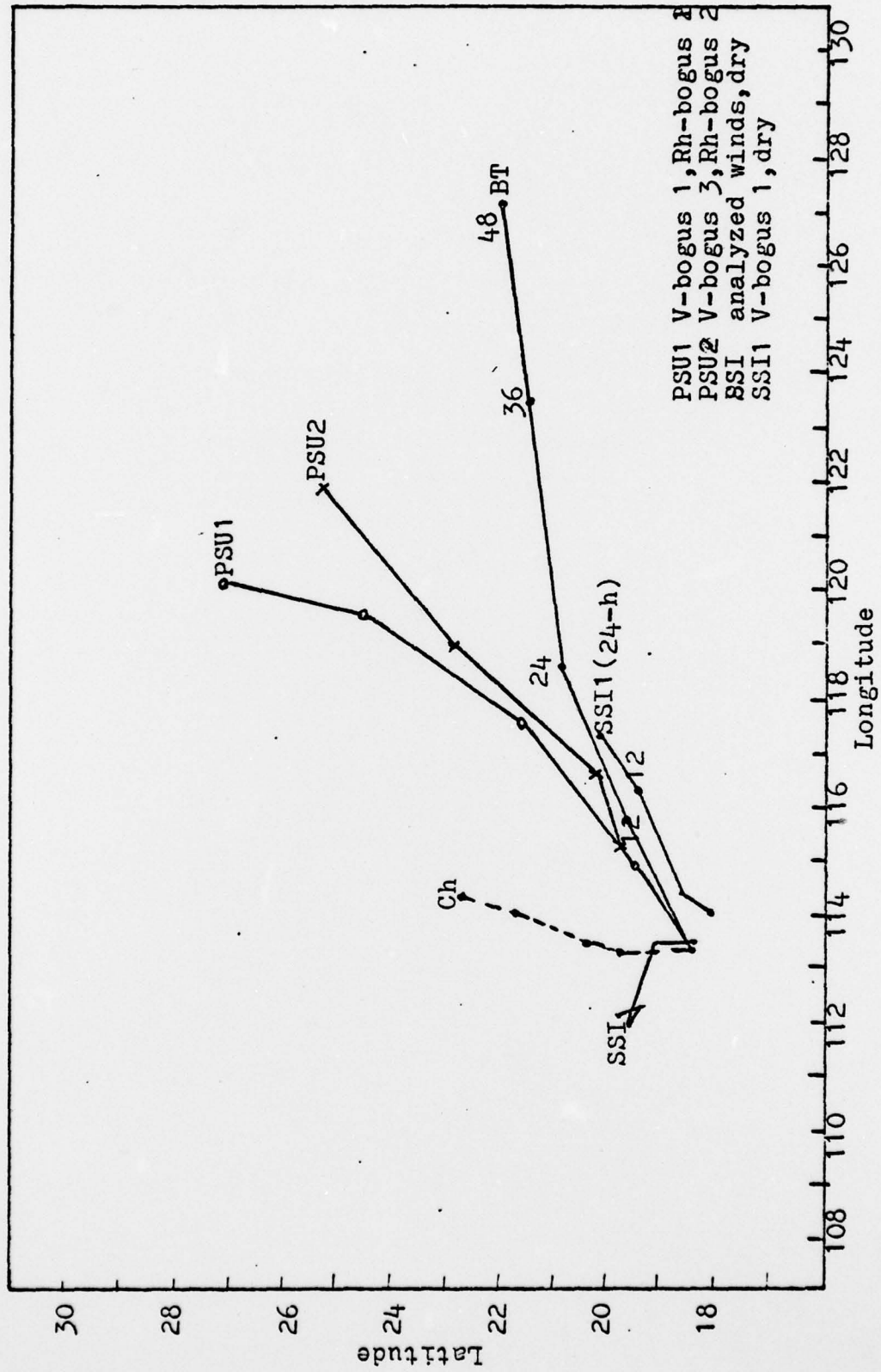


Fig. 18. Forecast tracks of Typhoon OLIVE(78042400) using the Penn State(PSU), split semi-implicit (SSI), and Channel(Ch) models.

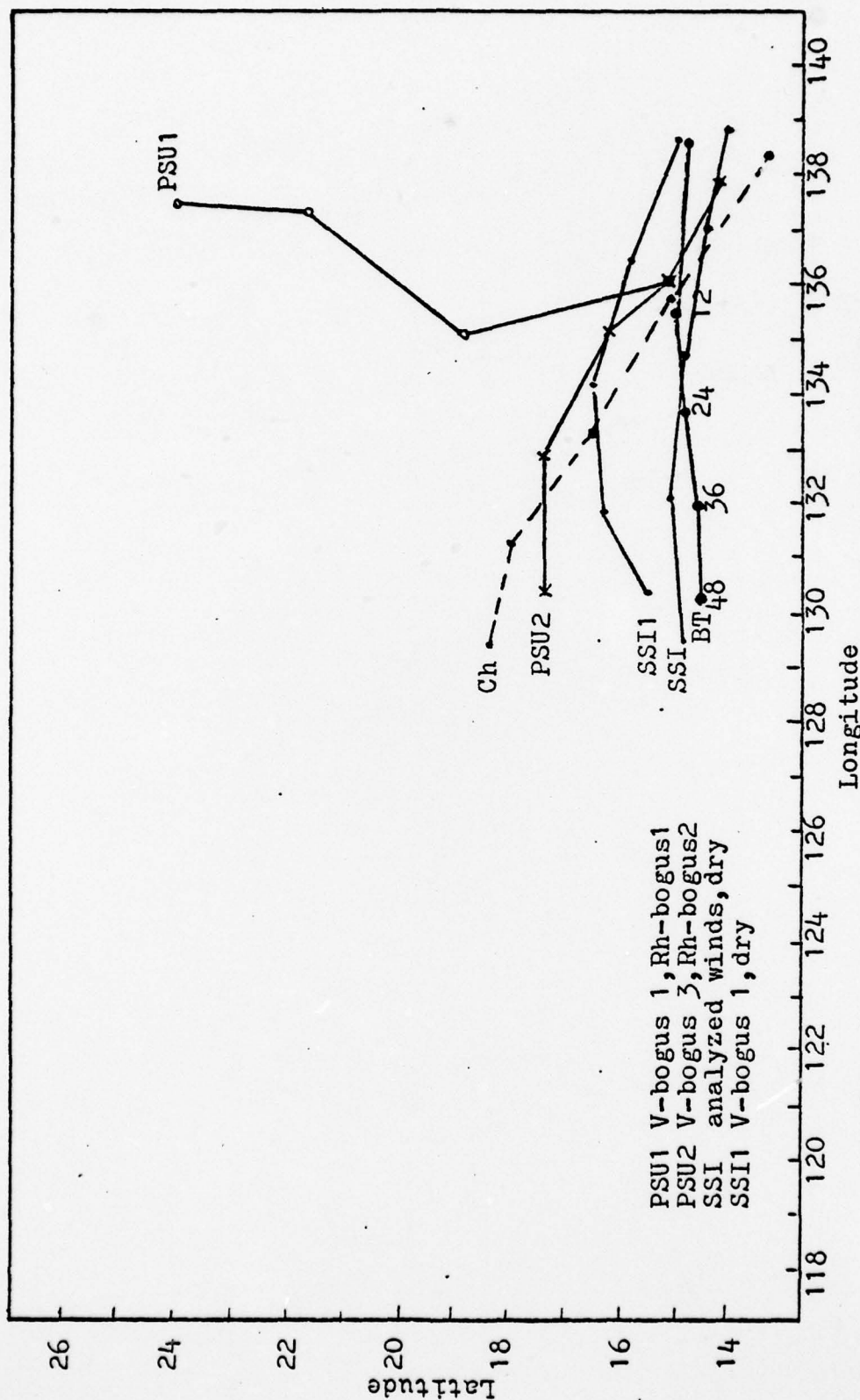


Fig. 19. Forecast tracks of Typhoon KIM(77110912) using the Penn State(PSU), split semi-implicit (SSI), and Channel(Ch) models.

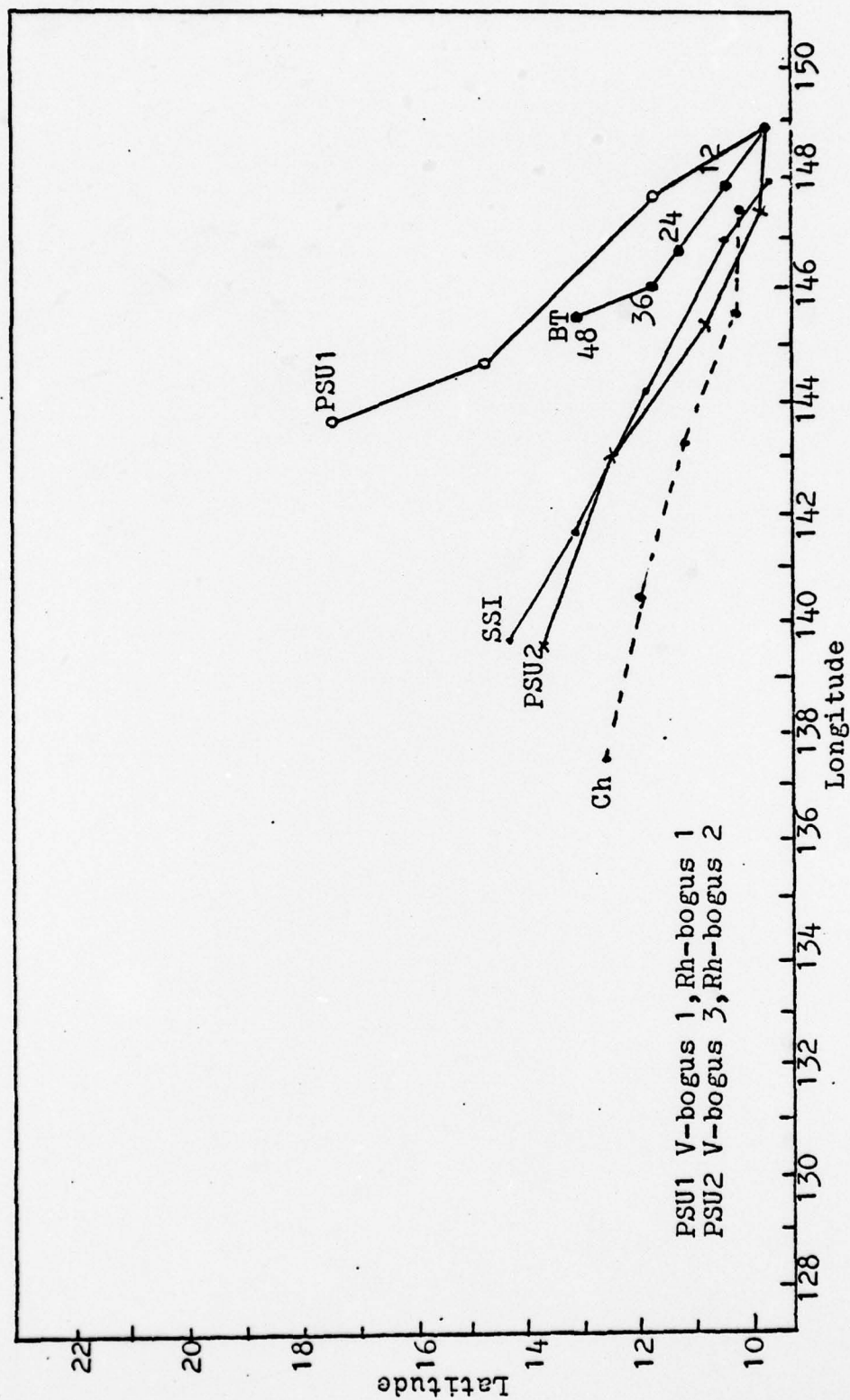


Fig.20. Forecast tracks of Typhoon PAMELA(76051900) using the Penn State(PSU), split semi-implicit (SSI), and Channel(Ch) models.

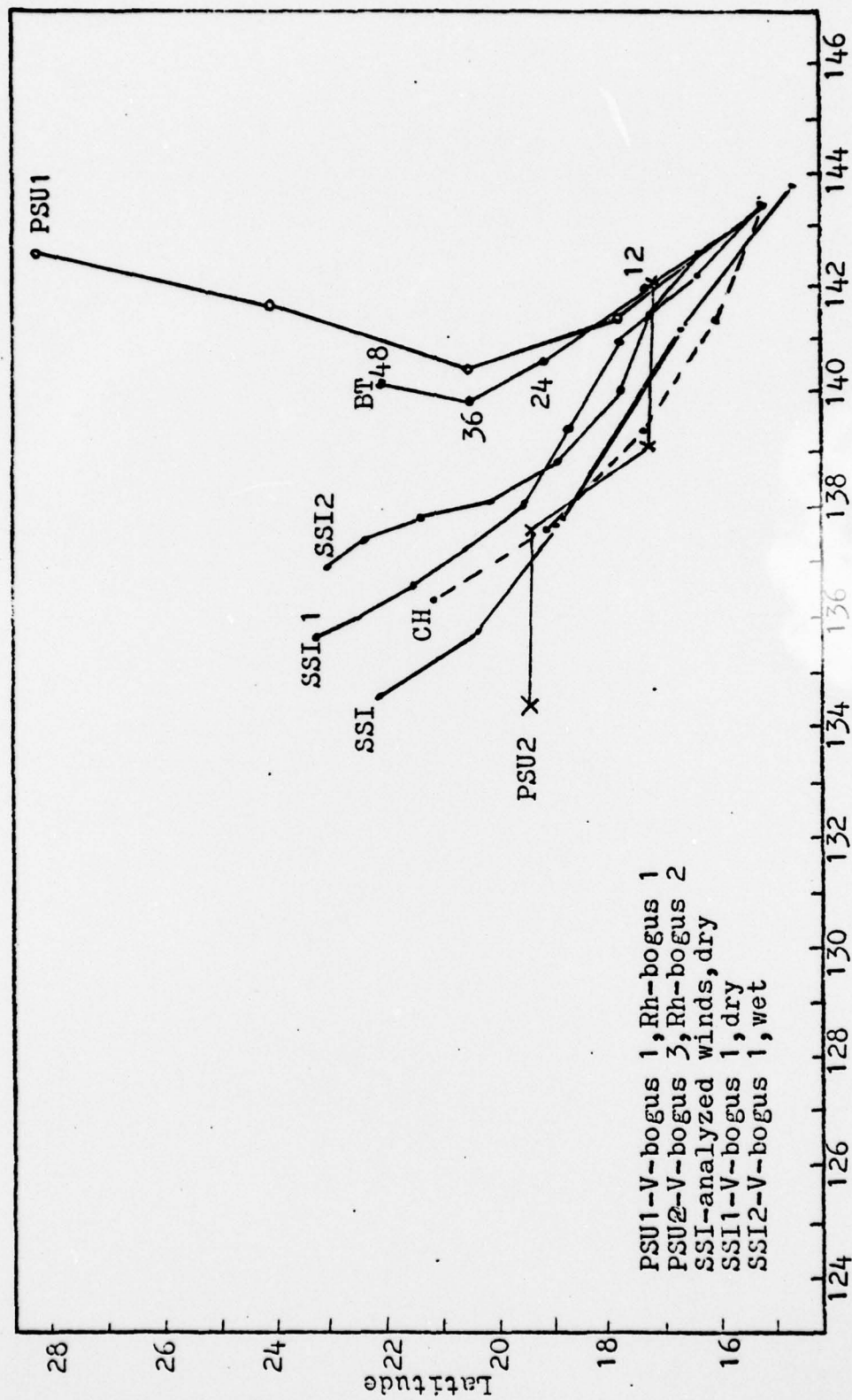


Fig. 21. Forecast tracks of Typhoon PAMELA(76052200) using the Penn State(PSU), split sem-implicit (SSI), and Channel(CH) models.



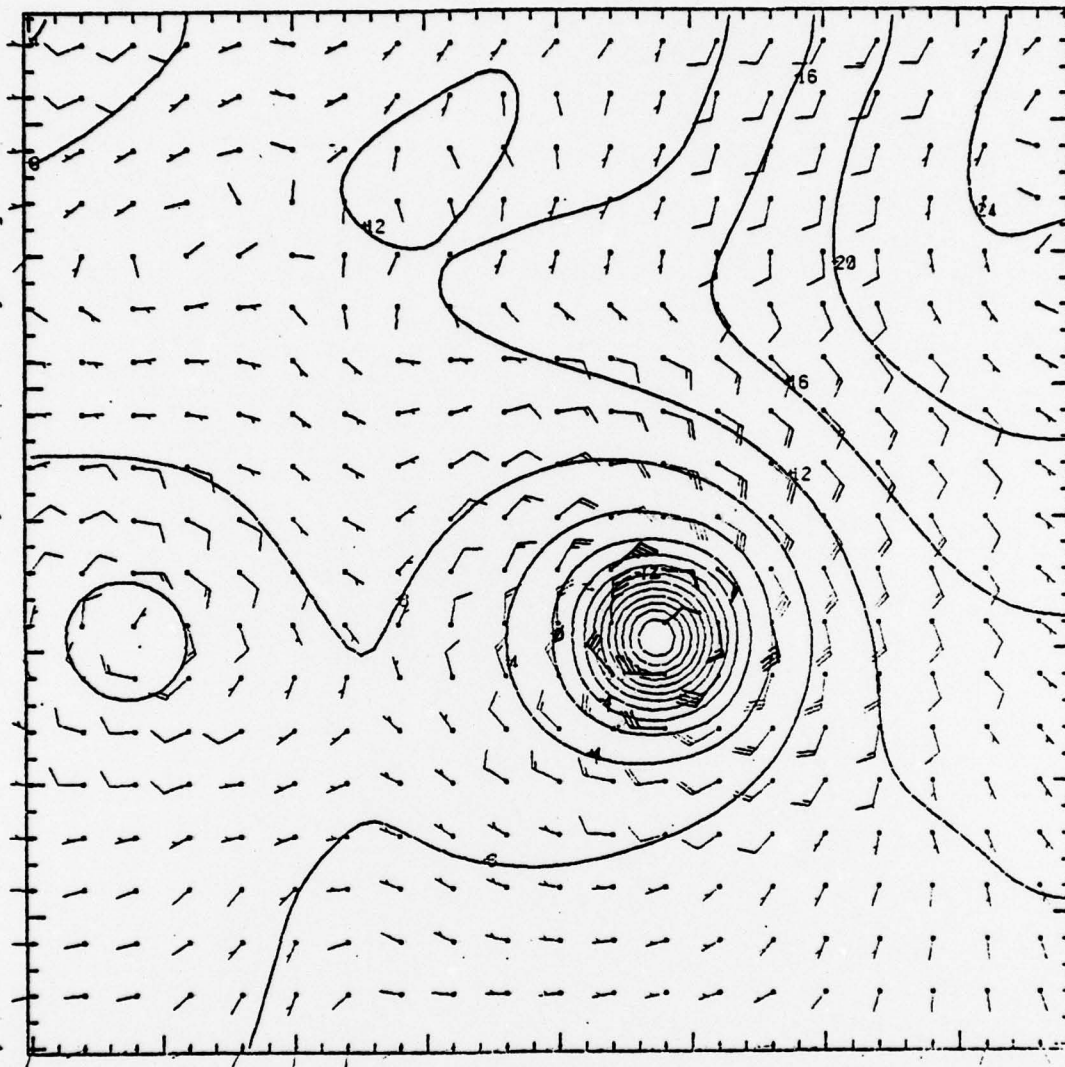


Figure 22. Typhoon PAMELA (76052200) initial  
SLP-1000 mb and winds ( $\text{m s}^{-1}$ ) at  
 $\sigma = .95$  using V-bogus 1

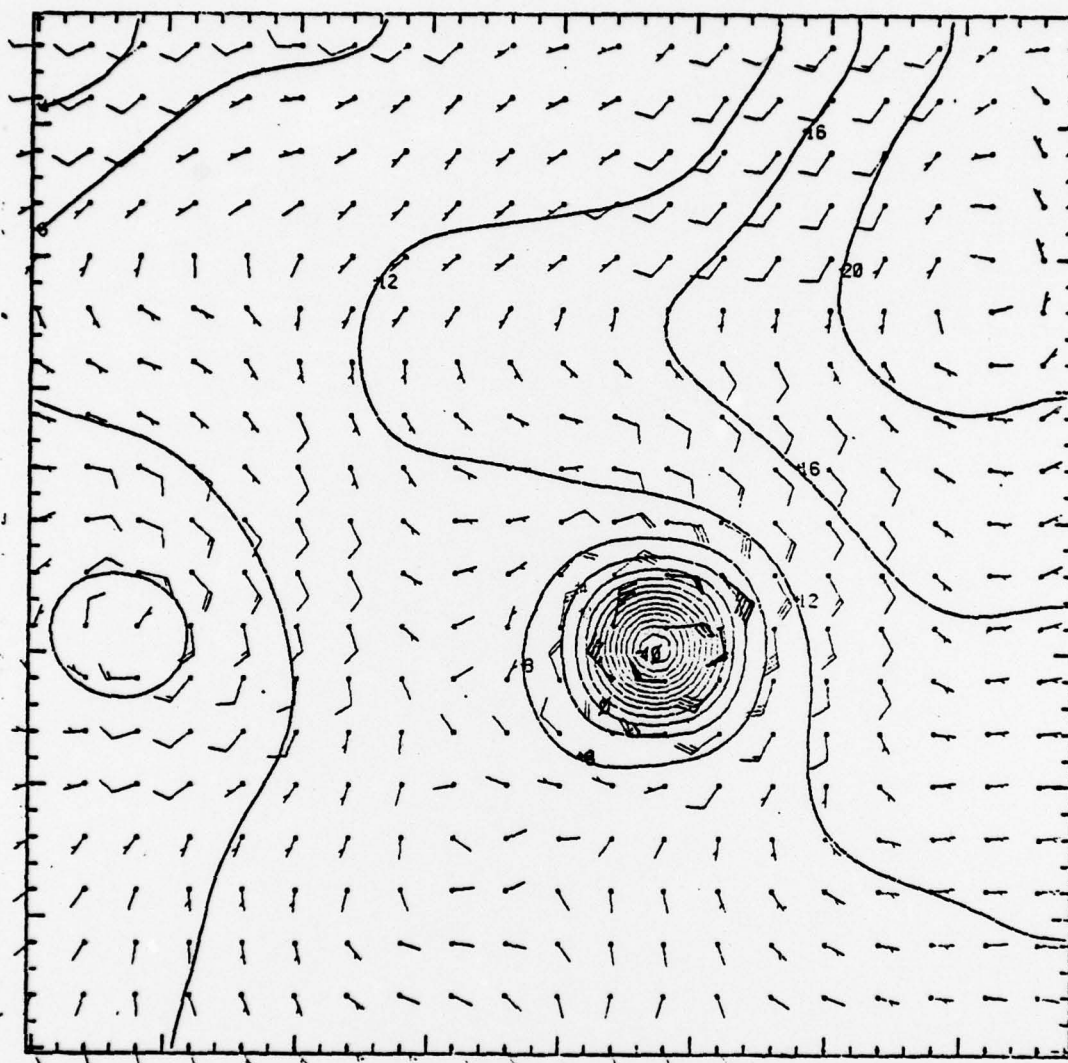


Figure 23. Typhoon PAMELA (76052200) initial SLP-1000 mb and winds ( $\text{m s}^{-1}$ ) using high intensity version of V-bogus 3 (V-bogus 4)

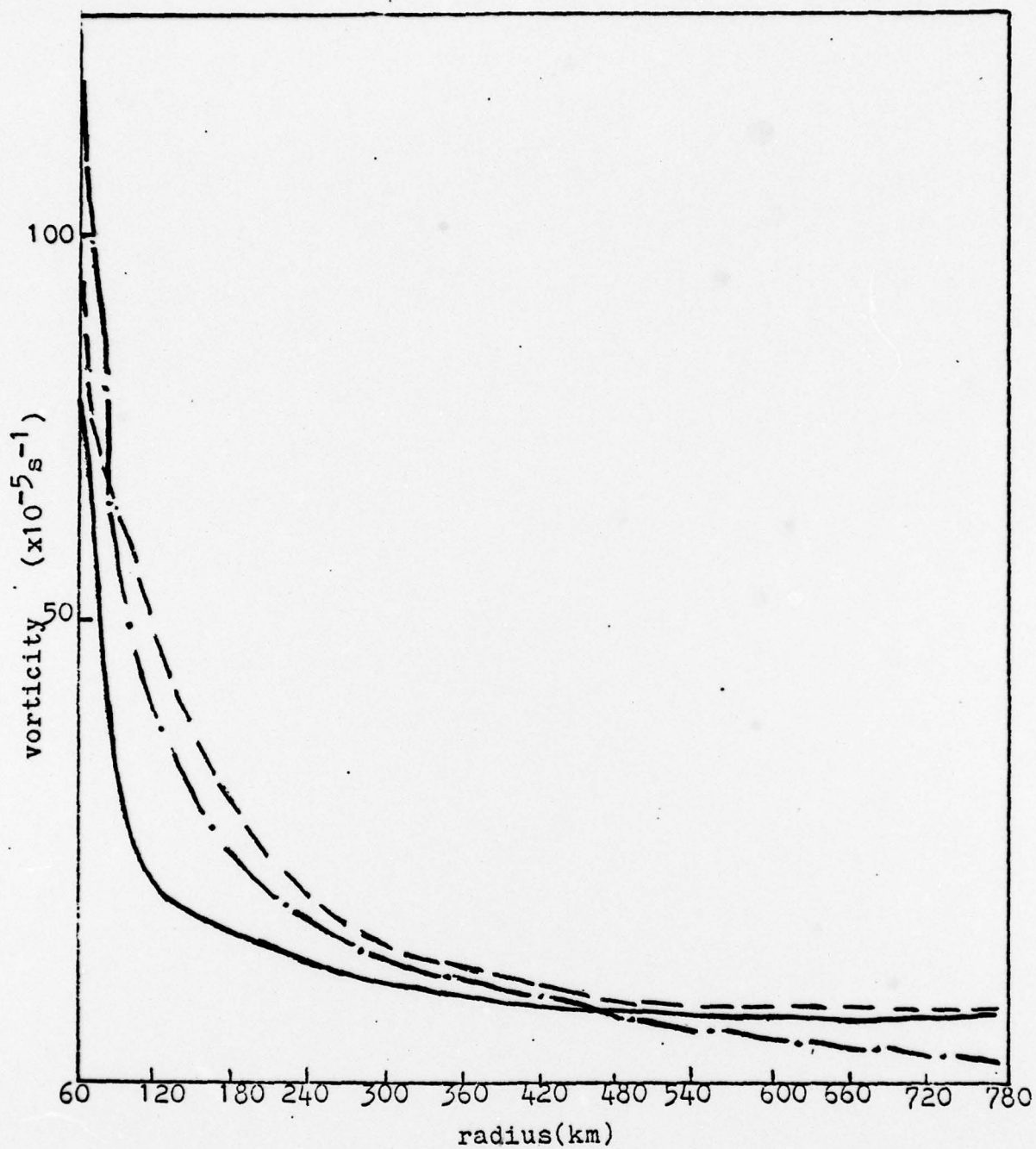


Fig. 24. Plot of vorticities produced by V-bogus 1, V-bogus 3 and the high intensity V-bogus 3 (V-bogus 4)

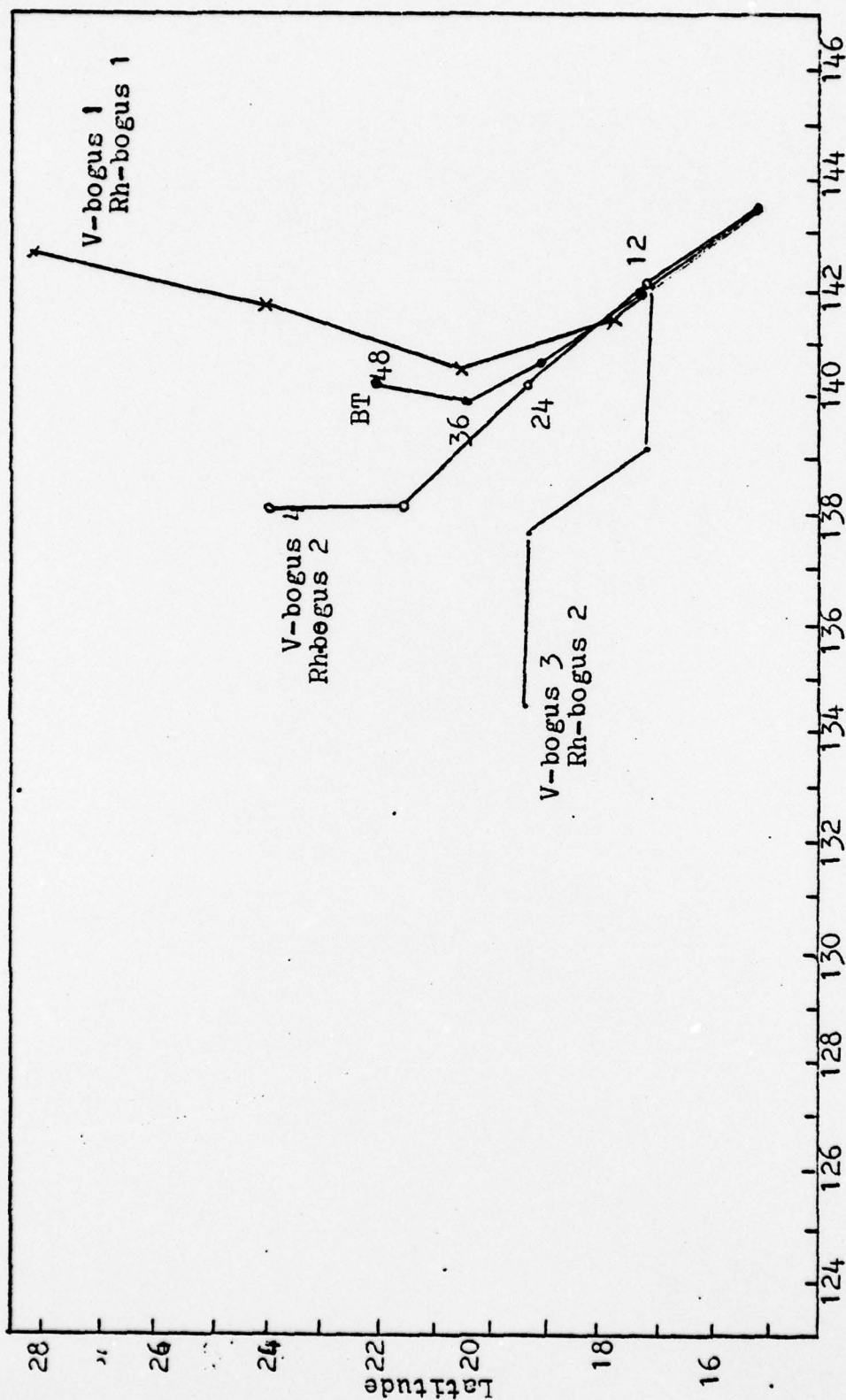


Fig. 25. Forecast tracks of PAMELA(76052200) using V-bogus 4 vs V-bogus 1 and V-bogus 3 in the Penn State (FSU) model.



## APPENDIX A

This appendix presents a brief comparison of the Penn State mesoscale model described in the accompanying paper to the Madala and Hodur split semi-implicit (SSI) tropical cyclone model and the Fleet Numerical Weather Central (FNWC) Channel model.

	Model		
	<u>Penn State</u>	<u>SSI</u>	<u>Channel</u>
Grid scheme	staggered	staggered	non-staggered
Finite differencing	centered space and time	centered space and time	centered space and time
Time scheme	explicit	explicit/semi-implicit	explicit
Horizontal resolution	120 km	60 km	205
grid size	40x40	51x51	32x24
Vertical levels	5-sigma levels	5-sigma levels	3-pressure levels
Boundary conditions	one-way interactive	one-way interactive	cyclic: east-west walls: north-south
Horizontal diffusion	fourth order	second order	-
Precipitation physics	Anthes cumulus parameter	Kuo cumulus parameter	bogused heating
Boundary layer physics	Deardorff's bulk parameterization	Deardorff's bulk parameterization	-
	Sensible heat flux at earth's surface	bogused heating	-

### LIST OF REFERENCES

1. Anthes, R.A., 1977: "A Cumulus Parameterization Scheme Utilizing a One-dimensional Cloud Model", Mon. Wea. Rev., 105, 270-286.
2. Anthes, R.A., 1978: Tests of a Mesoscale Model over Europe and the United States. Naval Postgraduate School Technical Report No. NPS 63-78004.
3. Anthes, R.A., and T.T. Warner, 1978: "Development of Hydrodynamic Models Suitable for Air Pollution and Other Meteorological Studies", Mon. Wea. Rev., 106, 1045-1078.
4. Deardorff, J.W., 1972: "Parameterization of the Planetary Boundary Layer for Use in General Circulation Models", Mon. Wea. Rev., 100, 93-106.
5. Hovermale, J.B., S.H. Scolnik, and D.G. Marks, 1976: Performance of the NMC Moveable Fine Mesh Model (MFM) Pertaining to Hurricane Prediction during the 1976 Hurricane Season. (Unpublished)
6. Jordan, C.L., 1958: "Mean Soundings for the West Indies Area", J. Meteor., 15, 91-97.
7. Madal, R.V., and R.M. Hodur, 1977: A Multi-layer Nested Tropical Cyclone Prediction Model in  $\sigma$  Coordinates. 11th Technical Conference on Hurricanes and Tropical Meteorology Conference Papers. 101-103.
8. Mihok, W.F., and D.E. Hinsman, 1977: Tropical Storm Forecasts Using the Fleet Numerical Weather Center (FNWC) Tropical Cyclone Model. 11th Technical Conference on Hurricanes and Tropical Meteorology Conference Papers. 401-404.
9. Perkey, D.J., and C.W. Kreitzberg, 1976: "A Time Dependent Lateral Boundary Scheme for Limited-area Primitive Equation Models", Mon. Wea. Rev., 104, 744-755.
10. Sheets, R.C., 1969: "Some Mean Hurricane Soundings", J. Appl. Meteor., 8, 134-146.

# INITIAL DISTRIBUTION LIST

	No. Copies
1. Defense Documentation Center Cameron Station Alexandria, Virginia 22314	2
2. Library, Code 0142 Naval Postgraduate School Monterey, California 93940	2
3. Dr. G. J. Haltiner, Code 63Ha Department of Meteorology Naval Postgraduate School Monterey, California 93940	1
4. Dr. R. L. Elsberry, Code 63Es Department of Meteorology Naval Postgraduate School Monterey, California 93940	8
5. LT. M. R. Hacunda DEFMAPSCOL (TSD-MC) Fort Belvoir, Virginia 22060	3
6. Dr. R. A. Anthes Department of Meteorology Pennsylvania State University University Park, Pennsylvania 16801	1
7. Department of Meteorology, Code 63 Naval Postgraduate School Monterey, California 93940	1
8. Commanding Officer Naval Environmental Prediction Research Facility Monterey, California 93940	1
9. Commanding Officer Fleet Numerical Weather Central Monterey, California 93940	1
10. Commanding Officer Fleet Weather Central/Joint Typhoon Warning Center COMNAVMARIANAS Box 12 FPO San Francisco 96630	1



11. Commander, Naval Oceanography Command 1  
National Space Technology Laboratories  
Bay St. Louis, Mississippi 39520
12. Mr. R. Hodur 1  
Naval Environmental Prediction Research  
Facility  
Monterey, California 93940